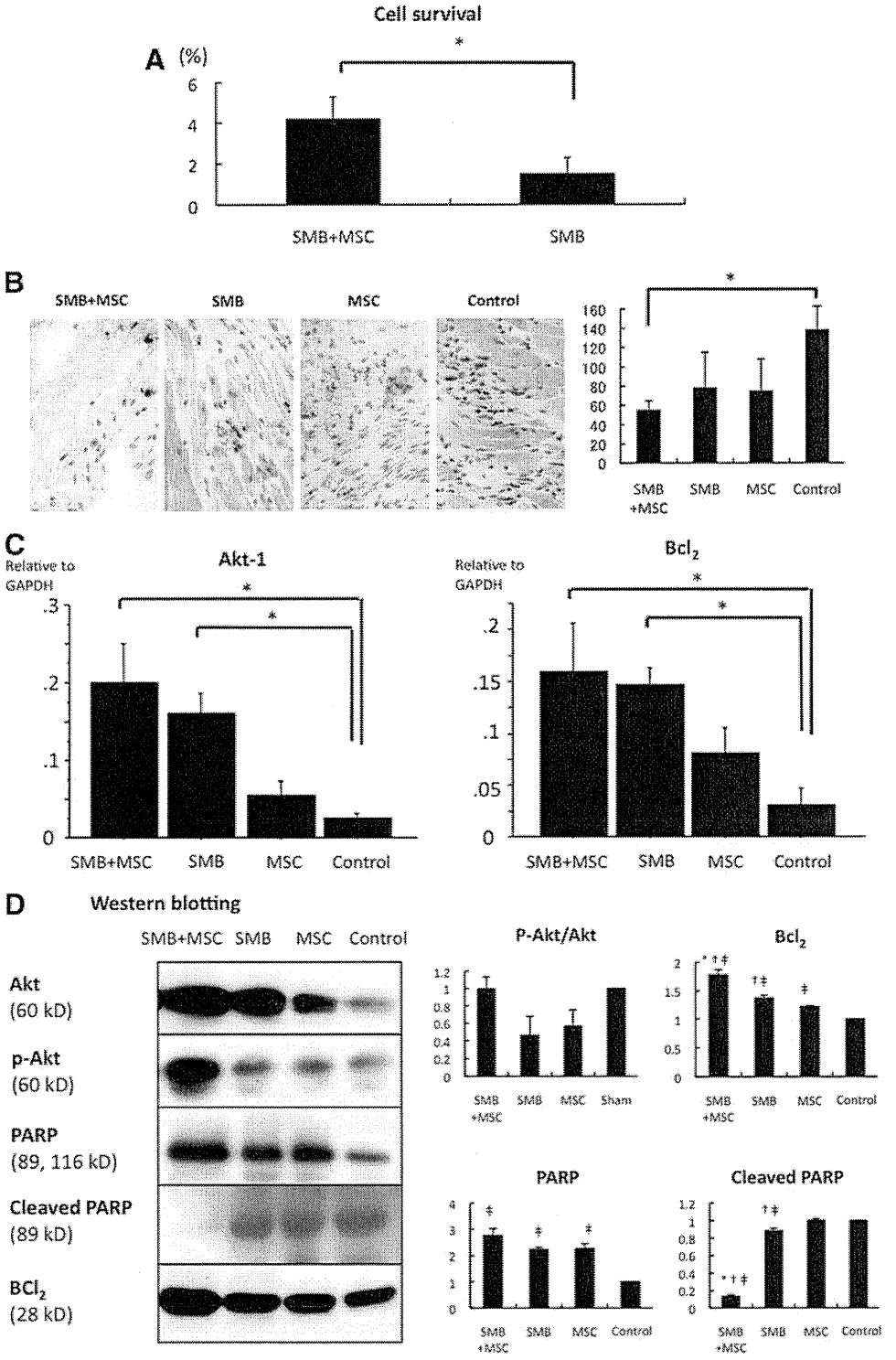

FIG. 6. Cell survival. **(A)** Survival of transplanted cells of rat origin was significantly greater in the SMB+MSC sheet group than in the SMB sheet group. $N = 4$ in each group. $^*p < 0.05$. **(B)** The number of terminal deoxynucleotidyl transferase-mediated dUTP nick end labeling (TUNEL)-positive myocytes was significantly lower in SMB+MSC group than in control. $N = 4$ in each group. $^*p < 0.05$. **(C)** Expressions of mRNA in the transplanted infarct area of hearts were determined by real-time PCR using rat-specific primers. The expressions of Akt-1 and Bcl_2 mRNA were significantly increased in the SMB+MSC sheet group compared with the other groups. $N = 4$ in each group. $^*p < 0.05$. **(D)** Western blotting showed that Bcl_2 was much more enhanced, and cleaved PARP was significantly downregulated in the SMB+MSC group. There was no significant difference in the ratio of phosphorylation of Akt over Akt. $N = 3$ in each group. $^*p < 0.05$ versus SMB. $^\dagger p < 0.05$ versus MSC. $^\ddagger p < 0.05$ versus control. Error bars = SD. Color images available online at www.liebertpub.com/tea

sheets' release of HGF and VEGF but not of IGF-1, bFGF, or SDF-1, *in vitro*. The transplantation of SMB-only cell sheets into the chronically ischemic failing rat heart resulted in reversed LV remodeling, including increased capillaries, attenuated collagen accumulation, and prolonged cell survival, which increased global functional recovery, mediated by the paracrine effects of upregulated HGF and VEGF in the myocardium.

Recent studies, including ours,[3–9] have suggested that a paracrine effect mediated by cytokines secreted from the transplanted cell sheets is a likely mechanism for the therapeutic effects on the myocardium, which was a focus of the present study. Here, we added h-MSCs to the cell sheets to enhance the potential performance of the transplanted r-SMB sheets. Our *in vitro* findings, that h-MSCs enhanced rat mRNA levels and the secretion of cytokines such as r-HGF

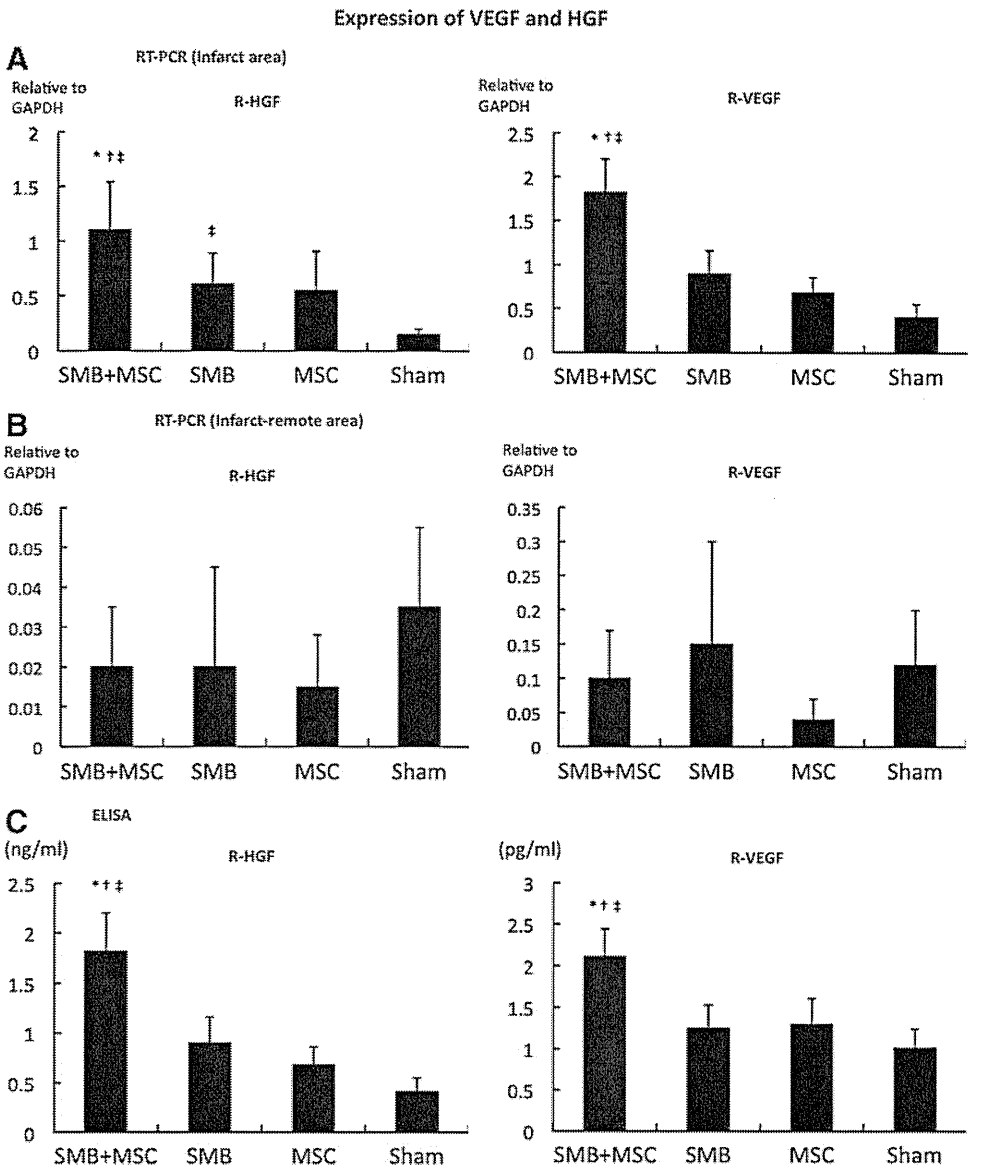

FIG. 7. Expression of VEGF and HGF is higher at the infarct area. **(A, B)** Levels of mRNA in the transplanted infarct and infarct-remote heart areas by real-time PCR using rat-specific primers. The HGF and VEGF mRNA expressions within the transplanted infarct area of the hearts were significantly increased in the SMB + MSC sheet group compared with the other groups. $N = 4$ in each group. $^{*}p < 0.05$ versus SMB. $^{\dagger}p < 0.05$ versus MSC. $^{\ddagger}p < 0.05$ versus sham. **(C)** Intramyocardial protein levels of HGF and VEGF, analyzed by ELISA, were significantly greater in the heart in the SMB + MSC sheet group compared with the other groups. $^{*}p < 0.05$ versus SMB. $^{\dagger}p < 0.05$ versus MSC. $^{\ddagger}p < 0.05$ versus control. Error bars = SD.

and r-VEGF from r-SMBs, suggested that transplanted co-cultured cell sheets would secrete r-HGF and r-VEGF *in vivo*. Although the exact mechanisms by which "feeder layers" support cell growth have not been elucidated, it is possible that h-MSCs enhance the r-SMBs directly (via cellular interaction) or indirectly (via secreted cytokines from the h-MSCs).[16] A more comprehensive examination aimed at differentiating these effects might help reveal how feeder layers work.

HGF and VEGF participate in many complex molecular and cellular mechanisms, and their signaling pathways have been intensively investigated *in vivo*.[3,9] SMBs or MSCs act as the natural supplier of both HGF and VEGF and provide feasible and safe sources for cell therapy in clinical applications. Indeed, SMBs and bone marrow-derived mesenchymal stem cell sheets can secrete growth factors (e.g., HGF and VEGF) into the myocardium and accelerate neovascularization in the damaged area.[5–8] More recent reports have revealed that angiogenesis induced by HGF or VEGF, an antifibrotic effect promoted by HGF, or the migration and survival of SMBs supported by VEGF,[17] could be beneficial to an impaired heart.[7,8] In addition, our data from a cytokine/chemokine multiplex immunology assay indicate that leptin may also be beneficial (e.g., by inducing angiogenesis though the Jak/STAT pathway).[18] Other cytokines may also contribute to the improvement of cardiac function by single-cell-type cell sheets in as-yet-undiscovered ways.

The mechanism by which the implanted cell sheet attenuates ventricular remodeling and improves cardiac function seems to depend on the cell sheet being placed over the scarred area of the myocardium and leads to repair of the anterior wall thickness, reduction of LV wall stress, and the improvement of ejection performance.[3] Previous studies indicated that the surviving myocardium and implanted cell sheet attenuate complex cellular and molecular events, including hypertrophy, fibrosis, apoptosis of the myocardium, and the pathological accumulation of extracellular matrix.[9] Similarly, the greater cellularity observed after cell-sheet

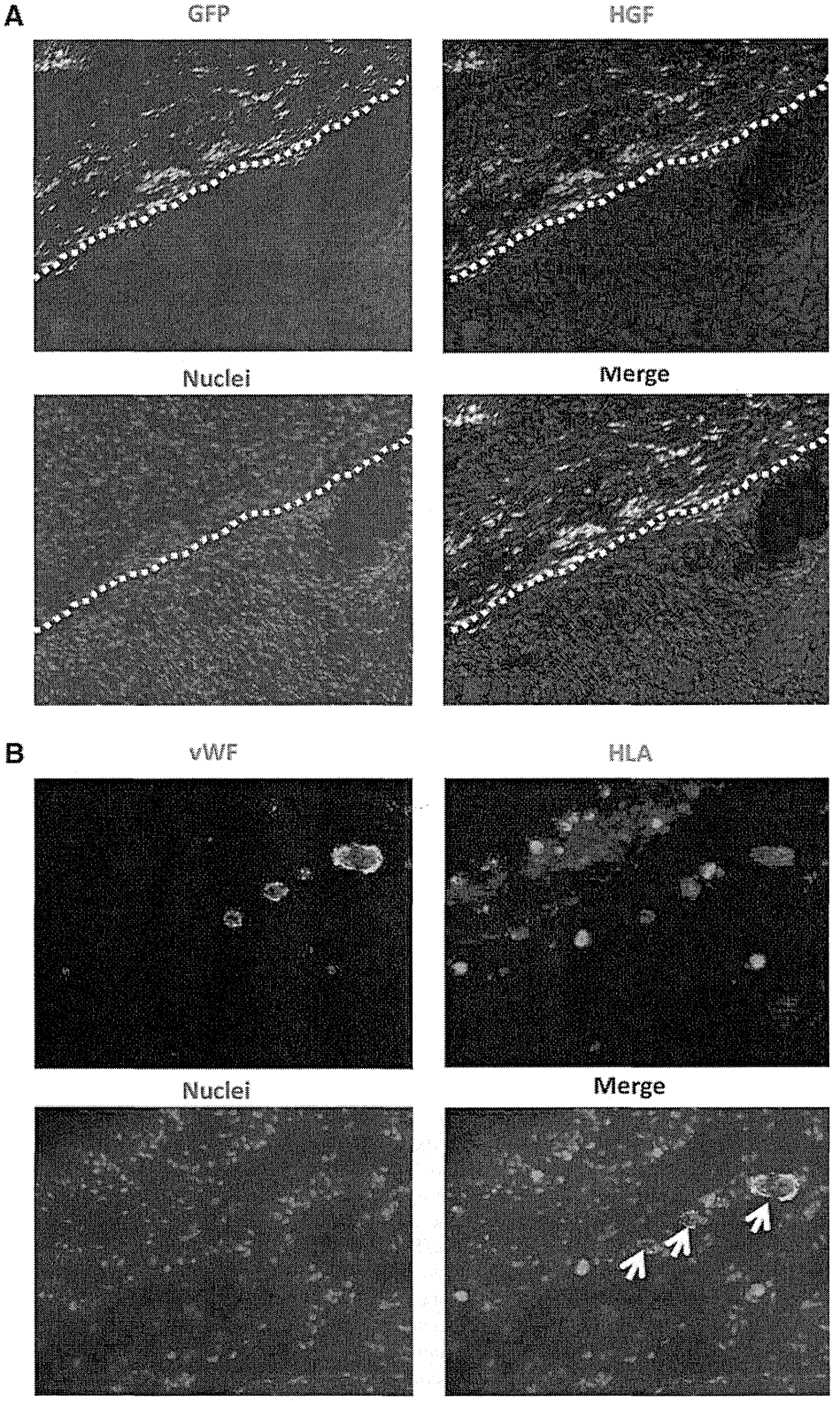

FIG. 8. Characterization of transplanted cells. **(A)** Cryosections were stained with an antibody to HGF to detect the distribution of SMB and HGF in the heart. HGF expressions and GFP-positive cells were found in the myocardium after transplantation of the SMB+MSC sheet. White broken line shows the border between the transplanted cell sheet and the host heart. Green indicates GFP; red, HGF; blue, nuclei. **(B)** Cryosections were stained with antibodies to human leukocyte antigen (HLA) and to von Willebrand factor (vWF). Human vWF-positive (white arrows) staining was observed in the host vessels in the h-MSC-transplanted group. Green indicates vWF; red, HLA; blue, nuclei. Color images available online at www.liebertpub.com/tea

treatment might have resulted from released SDF-1, which is related to cell migration, adhesion, and proliferation, by the transplanted cell sheet[19,20]

In this study, we performed additional investigations on the paracrine mechanism from a new perspective, by analyzing signaling pathways within the myocardium following cell-sheet transplantation because the signals induced by released paracrine mediators presumably activate phosphorylation cascades of signaling molecules. We found that STAT3 and Akt phosphorylations were significantly increased, and cleaved PARP was significantly downregulated, 24 h after the co-cultured cell-sheet implantation. Together

with our findings that vascular density was significantly enhanced, and myocardial apoptosis and fibrosis was significantly attenuated in the co-cultured group, it is possible that the co-cultured cell-sheet transplantation induced angiogenesis partially through the Jak/STAT signaling pathway[18] and that it prolonged cell survival by preventing apoptosis through PI-3K/Akt-mediated signaling, which is partially modulated by HGF.[21]

Although we emphasized combining SMBs with h-MSCs, some investigators have focused on different combinations of various cell sources. Sekine *et al.*[22] reported that cardiomyocytes co-cultured with endothelial cells induce greater numbers of capillaries, due to increased secretion of angiogenic growth factors.[22] Another report showed that a dermal fibroblast sheet co-cultured with endothelial progenitor cells was more effective than either single cell-type sheet for improving damaged heart function, accompanied by the inhibition of fibrotic tissue formation and the acceleration of neovascularization in the infarcted myocardium.[23] Thus, the paracrine effect may be improved by combining different cell sources; however, further investigation focused on determining the optimal combinations of cell sources is needed.

Regarding h-MSCs as a cell source, bone marrow-derived or adipose tissue-derived stem cells are reported to differentiate into mature endothelial cells and participate in blood vessel formation in the recipient heart.[24] The presence of endothelial capillary networks improves the survival and organization of implanted cells by maintaining a minimum intercapillary distance to provide oxygen and nutrients. Therefore, the presence of endothelial capillary networks may be partially correlated with cardiac function.

For future tissue engineering for cardiac therapy, the creation of thick cell-dense constructs with functional vessels may be essential. Capillary formation occurs via two basic vessel-constructing processes: angiogenesis, that is, the formation of new capillaries via sprouting or intussusception from pre-existing vessels, and vasculogenesis, which occurs in the developing embryo.[25] Here, the morphology of the vessel formation within myocardial tissues, including the diameter, composition, and fragility of vessel walls, suggested that improper vascularization may occur under pathological conditions. It is likely that not only biological factors but also physical stimuli such as flow and shear stress are required to mimic the *in vivo* environment and enable the formation of mature vascular networks.

A potential limitation of this study is that the exact number of transplanted cells was different in each group *in vivo*. Clinically, open-chest surgery is unlikely to gain easy acceptance except in certain situations; however, less invasive methods (e.g., intracoronary catheter-based procedures) might be technically difficult for carefully placing the cell sheets. Additionally, further studies that include longer timeframe than 8 weeks are needed to examine a longer term restoration of heart function post-MI. It is likely that the source of HGF is the transplanted SMB; however, it is unclear whether the source of other therapeutic cytokines is the transplanted cells, such as SMBs, MSCs, or both, or native cardiac cells.

In conclusion, we found that h-MSCs enhanced the paracrine effects of r-SMB sheets, thus enhancing angiogenesis, lowering fibrosis, inhibiting cellular hypertrophy, improving cardiac function, and prolonging cell survival in MI model rats. These observations of improved effects from this co-cultured cell sheet may lead to new regeneration therapies for heart failure following advanced cardiomyopathy that are superior to the conventional SMB-only cell-sheet technique.

Acknowledgments

We thank Dr. Eiji Kobayashi and Takashi Murakami for kindly providing the GFP transgenic Lewis rats. We thank Mr. Akima Harada, Mr. Shigeru Matsumi, and Mrs. Masako Yokoyama for their excellent technical assistance.

Sources of Funding: This study was supported by Grants for the Research and Development of the Myocardial Regeneration Medicine Program from the New Energy Industrial Technology Development Organization (NEDO), Japan. This research was supported by the Health and Labour Sciences Research Grants, Research on intractable diseases.

Disclosure Statement

T.S. is a consultant for CellSeed, Inc. T.O. is an Advisory Board Member in CellSeed, Inc., and the inventor/developer designated on the patent for temperature-responsive culture surfaces.

References

1. Menasche, P., Hagege, A.A., Scorsin, M., Puzet, B., Desnos, B., Schwartz, K., Vilquin, J.T., and Marolleau, J.P. Myoblast transplantation in heart failure. Lancet **357,** 279, 2001.
2. Hagege, A.A., Marolleau, J.P., Vilqiun, J.T., Alheritiere, A., Peyrard, S., Duboc, D., Abergel, E., Messas, E., Mousseaux, E., Schwartz, K., Desnos, M., and Menasche, P. Skeletal myoblast transplantation in ischemic heart failure: Long-term follow-up of the first phase I cohort of patients. Circulation **114,** I108, 2006.
3. Miyagawa, S., Roth, M., Saito, A., Sawa, Y., and Kostin, S. Tissue-engineered cardiac constructs for cardiac repair. Ann Thorac Surg **91,** 320, 2011.
4. Imanishi, Y., Miyagawa, S., Maeda, N., Fukushima, S., Kitagawa-Sakakida, S., Daimon, T., Hirata, A., Shimizu, T., Okano, T., Shimomura, I., and Sawa, Y. Induced adipocyte cell-sheet ameliorates cardiac dysfunction in a mouse myocardial infarction model: a novel drug delivery system for heart failure. Circulation **124,** S10, 2011.
5. Miyagawa, S., Saito, A., Sakaguchi, T., Yoshikawa, Y., Yamauchi, T., Imanishi, Y., Kawaguchi, N., Teramoto, N., Matsuura, N., Iida, H., Shimizu, T., Okano, T., and Sawa, Y. Impaired myocardium regeneration with skeletal cell sheets—a preclinical trial for tissue-engineered regeneration therapy. Transplantation **90,** 364, 2010.
6. Fujita, T., Sakaguchi, T., Miyagawa, S., Saito, A., Sekiya, N., Izutani, H., and Sawa, Y. Clinical impact of combined transplantation of autologous skeletal myoblasts and bone marrow mononuclear cells in patients with severely deteriorated ischemic cardiomyopathy. Surg Today **41,** 1029, 2011.
7. Sekiya, N., Matsumiya, G., Miyagawa, S., Saito, A., Shimizu, T., Okano, T., Kawaguchi, N., Matsuura, N., and Sawa, Y. Layered implantation of myoblast sheets attenuates adverse cardiac remodeling of the infarcted heart. J Thorac Cardiovasc Surg **138,** 985, 2009.
8. Memon, I.A., Sawa, Y., Fukushima, N., Matsumiya, G., Miyagawa, S., Taketani, S., Sakakida, S.K., Kondoh, H.,

Aleshin, A.N., Shimizu, T., Okano, T., and Matsuda, H. Repair of impaired myocardium by means of implantation of engineered autologous myoblast sheets. J Thorac Cardiovasc Surg **130,** 646, 2009.
9. Matuura, K., Honda, A., Nagai, T., Fukushima, N., Iwanaga, K., Tokunaga, M., Shimizu, T., Okano, T., Kasanuki, H., Hagiwara, N., and Komuro, I. Transplantation of cardiac progenitor cells ameliorates cardiac dysfunction after myocardial infarction in mice. J Clin Invest **119,** 2204, 2009.
10. Majumdar, M.K., Thiede, M.A., Mosca, J.D., Moorman, M., and Gerson, S.L. Phenotypic and functional comparison of cultures of marrow-derived mesenchymal stem cells (MSCs) and stromal cells. J Cell Physiol **176,** 57, 1998.
11. Richards, M., Fong, C.Y., Chan, W.K., Wong, P.C., and Bongso, A. Human feeders support prolonged undifferentiated growth of human inner cell masses and embryonic stem cells. Nat Biotechnol **20,** 933, 2002.
12. Ohkura, H., Matsuyama, A., Lee, C.M., Saga, A., Kakuta-Yamamoto, A., Nagao, A., Sougawa, N., Sekiya, N., Takekita, K., Shudo, Y., Miyagawa, S., Komoda, H., Okano, T., and Sawa, Y. Cardiomyoblast-like cells differentiated from human adipose tissue-derived mesenchymal stem cells improve left ventricular dysfunction and survival in a rat myocardial infarction model. Tissue Eng Part C Methods **16,** 417, 2010.
13. Pittenger, M.F., Mackay, A.M., Beck, S.C., Jaiswal, R.K., Douglas, R., Mosca, J.D., Moorman, M.A., Simonetti, D.W., Craig, S., and Marshak, D.R. Multilineage potential of adult human mesenchymal stem cells. Science **284,** 143, 1999.
14. Jiang, Y., Jahagirar, B.N., Reinhardt, R.L., Schwartz, R.E., Keene, C.D., Ortiz-Gonzales, X.R., Reyes, M., Lenrik, T., Lund, T., Blackstad, M., Du, J., Aldrich, S., Lisberg, A., Low, W.C., Largaespada, D.A., and Vertaille, C.M. Pluripotency of mesenchymal stem cells derived from adult marrow. Nature **418,** 41, 2002.
15. Inoue, H., Ohsawa, I., Murakami, T., Kimura, A., Hakamata, Y., Sato, Y., Kaneko, T., Takahashi, M., Okada, T., Ozawa, K., Francis, J., Leone, P., and Kobayashi, E. Development of new inbred transgenic strains of rats with LacZ or GFP. Biochem Biophys Res Commun **329,** 288, 2005.
16. Kirouac Dc, and Zandstra, P.W. Understanding cellular networks to improve hematopoietic stem cell expansion cultures. Curr Opin Biotechnol **17,** 538, 2006.
17. Germani, A., Di Carlo, A., Mangoni, A., Straino, S., Giacinti, C., Turrini, P., Biglioli, P., and Capogrosse, M.C. Vascular endothelial growth factor modulates skeletal myoblast function. Am J Pathol **163,** 1417, 2003.
18. Sierra-Honigmann, M.R., Nath, A.K., Murakami, C., García-Cardeña, G., Papapetropoulos, A., Sessa, W.C., Madge, L.A., Schechner, J.S., Schwabb, M.B., Polverini, P.J., and Flores-Riveros, J.R. Biological action of leptin as an angiogenic factor. Science **281,** 1683, 1998.
19. Hiesinger, W., Perez-Aguilar, J.M., Atluri, P., Marotta, N.A., Frederick, J.R., Fitzpatrick, J.R., 3rd, McCormick, R.C., Muenzer, J.R., Yang, E.C., Levit, R.D., Yuan, L.J., Macarthur, J.W., Saven, J.G., and Woo, Y.J. Computational protein design to reengineer stromal cell-derived factor-1a generates an effective and translatable angiogenic polypeptide analog. Circulation **124,** S18, 2011.
20. Frederick, J.R., Fitzpatrick, J.R., 3rd, McCormick, R.C., Harris, D.A., Kim, A.Y., Muenzer, J.R., Marotta, N., Smith, M.J., Cohen, J.E., Hiesinger, W., Atluri, P., and Woo, Y.J. Stromal cell-derived factor-1alpha activation of tissue-engineered endothelial progenitor cell matrix enhances ventricular function after myocardial infarction by inducing neovasculogenesis. Circulation **122,** S107, 2010.
21. Kakazu, A., Chandrasekher, G., and Bazan, H.E. HGF protects corneal epithelial cells from apoptosis by the PI-3K/Akt-1/Bad- but not the ERK 1/2-mediated signaling pathway. Invest Ophthalmol Vis Sci **45,** 3485, 2004.
22. Sekine, H., Shimizu, T., Hobo, K., Sekiya, S., Yang, J., Yamato, M., Kurosawa, H., Kobayashi, E., and Okano, T. Endothelial cell coculture within tissue-engineered cardiomyocyte sheets enhances neovascularization and improve cardiac function of ischemic hearts. Circulation **118,** S145, 2008.
23. Kobayashi, H., Shimizu, T., Yamato, M., Tono, K., Masuda, H., Asahara, T., Kasanuki, H., and Okano, T. Fibroblast sheets co-cultured with endothelial progenitor cells improve cardiac function of infarcted hearts. J Artif Organs **11,** 141, 2008.
24. Miyahara, Y., Nagaya, N., Kataoka, M., Yanagawa, B., Tanaka, K., Hao, H., Ishino, K., Ishida, H., Shimizu, T., Kangawa, K., Sano, S., Okano, T., Kitamura, S., and Mori, H. Monolayered mesenchymal stem cells repair scarred myocardium after myocardial infarction. Nat Med **12,** 459, 2006.
25. Risau, W. Mechanisms of angiogenesis. Nature **386,** 671, 1997.

Address correspondence to:
Yoshiki Sawa, MD, PhD
Department of Cardiovascular Surgery
Osaka University Graduate School of Medicine
Suita
Osaka 565-0871
Japan

E-mail: sawa-p@surg1.med.osaka-u.ac.jp

Received: September 2, 2012
Accepted: September 25, 2013
Online Publication Date: December 31, 2013

Circulation Journal
Official Journal of the Japanese Circulation Society
http://www.j-circ.or.jp

ORIGINAL ARTICLE
Regenerative Medicine

In Vivo Differentiation of Induced Pluripotent Stem Cell-Derived Cardiomyocytes

Tao Yu, BSc; Shigeru Miyagawa, MD, PhD; Kenji Miki, BSc; Atsuhiro Saito, PhD; Satsuki Fukushima, MD, PhD; Takahiro Higuchi, MD; Masashi Kawamura, MD; Takuji Kawamura, MD; Emiko Ito, PhD; Naomasa Kawaguchi, PhD; Yoshiki Sawa, MD, PhD; Nariaki Matsuura, MD, PhD

Background: Induced pluripotent stem cells (iPSCs) hold promise for a new era in treating heart failure. However, the functional microstructure of iPSC-derived cardiomyocytes (iPSC-CMs) and their ability to attach to the extracellular matrix of the recipient myocardium require further elucidation. Thus, we analyzed the functional microstructure and adhesion molecules of iPSC-CM.

Methods and Results: Immunostaining analysis showed that iPSC-CMs were similar to neonatal cardiomyocytes (CMs) in expressing the cytoskeletal proteins myosin heavy chain (MHC), myosin light chain (MLC) 2a, MLC2v, and especially β-MHC (a neonatal CM marker), as well as the adhesion molecules N-cadherin, α7-integrin, dystrophin, α-dystroglycan, α-sarcoglycan, and laminin-α2. Electron microscopy showed abundant myofibrillar bundles with transverse Z-bands and a developed mitochondrial structure in both iPSC-CMs and neonatal CMs, although the iPSC-CMs contained fewer mitochondria with lower-density cristae. When transplanted from in vitro conditions to nude rat hearts, iPSC-CMs acquired the ability to express α-MHC, a molecule specific to adult CMs. Mechanical stretch or stimulation by insulin-like growth factor-1 enhanced the α-MHC expression in iPSC-CMs in vitro.

Conclusions: Our findings in vitro and in vivo indicate that CMs derived from iPSCs contain cardiac-specific organelles and adhesion systems. These results indicate that iPSC-derived CMs may be useful in new cell therapies for heart failure. (*Circ J* 2013; **77:** 1297–1306)

Key Words: Adhesion molecules; Cardiomyocyte differentiation; Cytoskeleton; Induced pluripotent stem cells; Ultrastructure

Despite medical advances, end-stage heart failure is still a life-threatening disorder.[1,2] New treatments for ischemic heart disease, including thrombolytic agents and percutaneous angioplasty, have not been proven to replace scar tissue with functional contractile cardiomyocytes (CMs), and it is still difficult to improve the quality of life or prognosis for patients with end-stage heart failure.[3–5] Cell therapy has been introduced as a promising new treatment. The initial clinical applications, involving myoblast or bone marrow cell transplants, modestly improved cardiac performance through (mainly) paracrine effects rather than through differentiation of the transplanted cells into functional CMs.[6–8] To contribute directly to cardiac function, somatic tissue-derived stem or progenitor cells, such as c-kit+, Sca-1+, and mesenchymal stem cells have been used to treat heart failure. However, these cells were also found to improve cardiac function through paracrine effects; CM-specific markers have not been detected in most of the implanted cell populations.[9,10]

Editorial p1154

Research into "true" CMs, which have specific molecular phenotypes and are contractile both in vitro and in vivo, has generated a great deal of enthusiasm. Experimentally developed embryonic stem cells and induced pluripotent stem cells (iPSCs) are expected to provide the basis for new cell therapies.[11–13] CMs differentiated from these stem cells not only contract in vitro, but also express specific proteins appropriately. These CMs are considered to have good in vivo transplantation potential for both survival and function.[14,15] However, no studies have demonstrated that these cells have the necessary molecular patterns and microstructure, such as the

Received August 7, 2012; revised manuscript received November 25, 2012; accepted December 26, 2012; released online February 8, 2013 Time for primary review: 21 days

Division of Cardiovascular Surgery, Department of Surgery, Osaka University Graduate School of Medicine, Suita (T.Y., S.M., K.M., S.F., T.H., M.K., T.K., E.I., Y.S.); Department of Molecular Pathology, Osaka University Graduate School of Medicine and Health Science, Suita (T.Y., N.K., N.M.); and Medical Center for Translational Research, Osaka University Hospital, Suita (A.S.), Japan

Mailing address: Nariaki Matsuura, Professor, MD, PhD, Department of Molecular Pathology, Osaka University, Graduate School of Medicine and Health Sciences, 1-7 Yamada-oka, Suita 565-0871, Japan. E-mail: matsuura@sahs.med.osaka-u.ac.jp

ISSN-1346-9843 doi:10.1253/circj.CJ-12-0977

CM-specific structural proteins or mitochondria found in differentiated CMs, or that they have the ability to attach to the damaged heart after heterogeneous implantation.

The physiological stimulus of mechanical stretch is thought to be required for cardiac development and growth, and for the regular arrangement of CMs that creates effective heart contractions.[16–19] Cells in the cardiovascular system are constantly subjected to mechanical forces from the pulse of blood flow and shear stress in the beating heart. Mechanical stretch modulates growth, apoptosis, electric remodeling, autocrine and paracrine effects, and alterations in gene expression in cardiac myocytes.[20] Insulin-like growth factor-1 (IGF-1) and other growth factors are also important for cardiac development, maturation, and survival.[21,22]

In this study, we hypothesized that CMs derived from iPSCs (iPSC-CMs) might contain sufficient of the cardiac-specific organelles to restore the damaged heart after in vivo implantation, as well as adhesion systems to enable them to attach to and function in extracellular matrices after heterogeneous implantation into the heart. We studied phenotypic changes in transplanted iPSC-CMs in vivo, as well as the effect of growth factor stimulation or mechanical stretch on these cells in vitro.

Methods

Cell Culture

CMs WERE derived from the germline-competent mouse iPSC lines 20D-17 and 256H18[23,24] (generously donated by Professor S Yamanaka, Kyoto University, Japan). The 20D-17 cell line, which carries a Nanog promoter-driven green fluorescent protein, internal ribosome entry site, and puromycin-resistance gene (Nanog-iPSCs), was maintained as previously described. The 256H18 cell line, which was established by introducing only Oct3/4, Sox2, and Klf4 (without c-Myc), expressed red fluorescent protein (DsRed) constitutively. The iPSCs were cultured and maintained on feeder layers of mitomycin C-treated mouse embryonic fibroblasts (MEFs; Chemicon, Billerica, MA, USA) in Dulbecco's Modified Eagle Medium (DMEM; Nacalai Tesque, Kyoto, Japan) containing 15% fetal bovine serum (FBS; Biofill, Victoria, Australia), 100 μmol/L nonessential amino acids (NEAA, Invitrogen, Tokyo, Japan), 2 mmol/L L-glutamine (Invitrogen), 0.1 mmol/L 2-mercaptoethanol (Invitrogen), 50 U/ml penicillin, 50 mg/ml streptomycin (Invitrogen), and 1,000 U/ml recombinant leukemia inhibitory factor (LIF; Chemicon). The medium was replenished daily. MEFs were grown in an incubator at 37°C in 5% CO_2, in a medium containing high-glucose DMEM supplemented with 10% FBS, 1 mmol/L L-glutamine, 50 U/ml penicillin, and 50 mg/ml streptomycin. The medium was replenished daily. As the MEFs reached confluence, they were exposed to 50 mg/ml mitomycin C (Wako, Osaka, Japan) for 2.25 h. They were then washed in phosphate-buffered saline (PBS), trypsinized (0.05% Trypsin-EDTA; Invitrogen), plated at 75,000 cells/cm^2 on gelatin-coated tissue culture dishes as a feeder layer, and incubated overnight before plating the iPSCs.

Differentiation of iPSCs to Beating CMs

The iPSCs were trypsinized to prepare a single-cell suspension, and then counted. For myocardial differentiation, 500 iPSCs were resuspended in 30-μl aliquots of differentiation medium containing DM and a growth medium lacking LIF. Cells were cultured in 96-well HydroCell plates (CellSeed, Tokyo, Japan) for 2 days. On day 2, an additional 30 μl of DM containing 4 μmol/L 6-bromoindirubin-3'-oxime (a glycogen synthase kinase-3β inhibitor) (BIO, Calbiochem, Darmstadt, Germany) was added to each well.[25,26] On day 5, embryoid bodies (EBs) were plated individually onto gelatin-coated dishes, and on day 8, these were differentiated in serum-free modified eagle medium (MEM; Invitrogen) with insulin-transferrin-selenium-X (Invitrogen). From day 10 onward, areas of cells contracting could be observed in the iPSC EBs.

Sheet Formation of iPSC-Derived CMs

On day 5 (**Figure 1A**), EBs were plated onto 12-well temperature-responsive culture dishes (provided by Professor Okano, Tokyo Women's Medical University) at 37°C with the number of EBs adjusted to 20 per well; thereafter, on day 8, EBs were differentiated in the serum-free MEM with insulin-transferin-selenium-X (Invitrogen) and from day 10, areas of cells contracting could be observed in the EBs of the iPSCs. On day 19 the dishes were placed in a refrigerator set at 20°C, a few minutes after the iPSC-derived CM sheets had detached spontaneously from the dishes surface.[27]

Neonatal Mouse CM Isolation

Hearts were excised from day-old female mice (C57BL/6JJcl; Crea, Osaka, Japan) and placed immediately into cold Hanks Balanced Salt Solution (HBSS). The blood vessels and atria were removed, and the remaining right and left ventricular tissues were minced, washed with HBSS, and subjected to sequential digestion with 1% collagenase type II (Invitrogen)/HBSS solution at 37°C for 10 min, with 4 repetitions. The fragments were then collected, filtered through a cell strainer, centrifuged at 3,000 rpm for 10 min, placed in 60-mm-diameter dishes, and cultured in DMEM/Ham's F-12 (Invitrogen) supplemented with 10% FBS, 2 mmol/L glutamine, 100 U/ml penicillin, and 100 μ/ml streptomycin.

Reverse Transcription Polymerase Chain Reaction (RT-PCR)

Total RNA was extracted using an RNeasy Mini Kit (Qiagen, Valencia, CA, USA) from mouse iPSC-derived EBs on days 6, 8, 12, and 19; cDNA was synthesized using the Super Script III First-strand Synthesis System (Invitrogen). PCR was performed with KOD-plus (Toyobo, Osaka, Japan). PCR conditions included denaturation at 94°C for 30 s, annealing at 60°C for 30 s, and extension at 55°C for 1 min for 35 cycles, with a final extension at 72°C for 7 min. Glyceraldehyde-3-phosphate dehydrogenase was used as an internal control. Primer sequences are listed in **Table 1**.

Western Blotting

EBs at 6, 8, 12, and 19 days were lysed in a buffer containing 20 mmol/L Tris-HCl (pH 7.4), 100 mmol/L NaCl, 5 mmol/L EDTA, 1.0% Triton X-100, 10% glycerol, 0.1% SDS, 1.0% deoxycholic acid, 50 mmol/L NaF, 10 mmol/L $Na_3P_2O_7$, 1 mmol/L Na_3VO_4, 1 mmol/L phenylmethylsulfonyl fluoride, 10 mg/ml aprotinin, and 10 mg/ml leupeptin. Sample proteins were separated on SDS-polyacrylamide gels (8–12%) and transferred to nitrocellulose membranes. The membranes were blocked with milk for 1 h, incubated overnight with primary antibody (**Table 2**), washed, incubated with secondary antibody (anti-rabbit goat IgG; Dako, Tokyo, Japan) for 1 h, and visualized using chemiluminescent substrate. Light emission was detected by autoradiography and quantified using an image-analysis system (Bio-Rad, Tokyo, Japan).

Immunofluorescent Staining

Neonatal or iPSC-derived CMs were fixed with 4% paraformaldehyde at room temperature for 20 min, washed 3 times

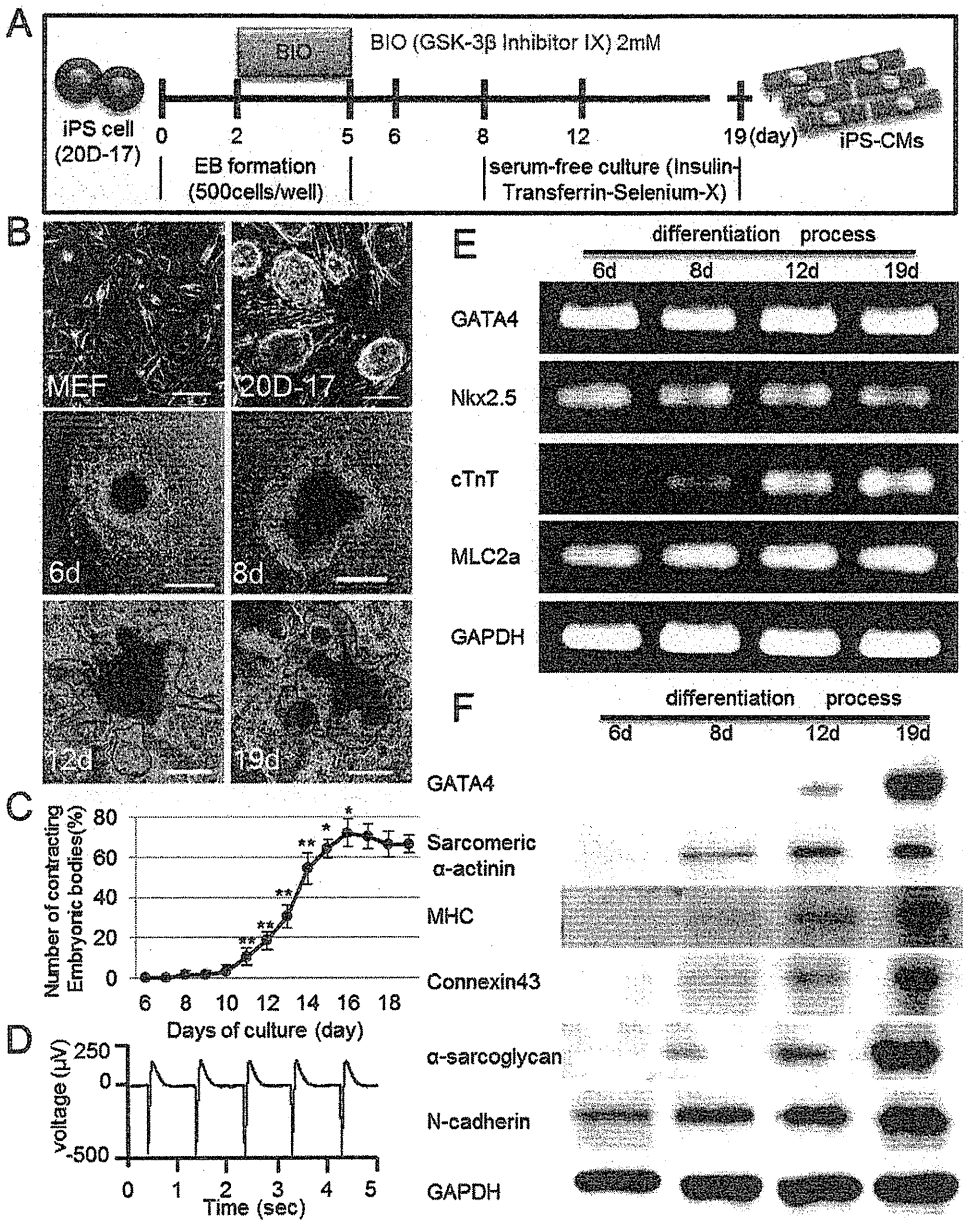

Figure 1. Differentiation of induced pluripotent stem cells (iPSCs) into cardiomyocytes. (**A**) Protocol for in vitro differentiation of iPSCs into cardiomyocytes. (**B**) Serial morphological changes during iPSC differentiation: iPSCs (20D-17) on a feeder layer (MEFs) can be seen as undifferentiated embryoid bodies (EBs) until day 5, when the EBs were placed individually on gelatin-coated dishes. On days 6 and 8, there were no areas of beating cells areas, but under the conditions of serum-free medium with insulin-transferrin-selenium-X starting on day 8, areas of beating differentiated cells (inside red line) were detected on days 12 and 19. Scale bars=100 μm. (**C**) Percentage of spontaneously beating EBs with the differentiation process. (**D**) Field-potential recordings of replated beating iPSC-derived cardiomyocyte (iPSC-CM) colonies, measured with the MED 64 system. (**E**) Reverse transcription polymerase chain reaction analysis of cardiac marker gene expression (GATA4, Nkx2.5, Cardiac Troponin T, and MLC2a) during the differentiation of iPSCs into cardiomyocytes (days 6–19). Glyceraldehyde-3-phosphate dehydrogenase (GAPDH) was used as a loading control. (**F**) Western blot analysis of the cardiac-specific proteins GATA4, sarcomeric α-actinin, MHC, connexin43, α-sarcoglycan, and N-cadherin from days 6 to 19. GAPDH was used as a loading control. *P<0.05, **P<0.01.

with PBS, permeabilized with 0.3% Triton X-100 (PBST, Nacalai Tesque) for 20 min, and blocked with 3% bovine serum albumin (BSA) in PBST for 1 h. The samples were incubated overnight at 4°C with a primary antibody (**Table 2**). The secondary antibody, Alexa Fluor 488 anti-rabbit goat IgG (1:1,000; Invitrogen) or Alexa Fluor 488 rabbit anti-rat IgG (1:1,000; Invitrogen), was applied to the sections for 1 h at room temperature. To visualize the F-actin cytoskeleton, cells were stained using Alexa Fluor 594 phalloidin (1:40; Invitrogen). Nuclei were stained with DAPI (Invitrogen, 1:1,000 dilution)

Table 1. Primers for Reverse Transcription Polymerase Chain Reaction

Gene	Direction	Sequences
GATA4	Forward	CTC CAT GTC CCA GAC ATT CAG TAC T
	Reverse	GAT TAT GTC CCC ATG ACT GTC AGC
Nkx2.5	Forward	CAG TGG AGC TGG ACA AAG CC
	Reverse	TAG CGA CGG TTC TGG AAC CA
cTroponin T	Forward	GCGGAAGAGTGGGAAGAGACA
	Reverse	CCACAGCTCCTTGGCCTTCT
MLC-2a	Forward	CCC ATC AAC TTC ACC GTC TTC CT
	Reverse	AGA GAA CTT GTC TGC CTG GGT CA
GAPDH	Forward	AGT ATG ACT CCA CTC ACG GCA A
	Reverse	TCT CGC TCC TGG AAG ATG GT

Table 2. Antibodies Used for Western Blot Studies and Immunostaining Studies

Antibody specificity	Source	Clonality	Dilution used
Western blot studies			
Anti-GATA4	Santa Cruz	Polyclonal	1:1,000
Anti-sarcomeric α-actinin	Abcam	Polyclonal	1:2,000
Anti-MHC	Abcam	Monoclonal	1:1,000
Anti-connexin43	Sigma	Monoclonal	1:2,000
Anti-α-sarcoglycan	Santa Cruz	Polyclonal	1:1,000
Anti-N-cadherin	Abcam	Polyclonal	1:1,000
Anti-GAPDH	Santa Cruz	Monoclonal	1:2,000
Immunostaining studies			
Anti-MHC	Abcam	Monoclonal	1:100
Anti-αMHC	Abcam	Monoclonal	1:100
Anti-βMHC	Sigma	Monoclonal	1:100
Anti-MLC-2a	Synaptic Systems	Monoclonal	1:100
Anti-MLC-2v	Synaptic Systems	Monoclonal	1:100
Anti-N-cadherin	Abcam	Polyclonal	1:100
Anti-α7-integrin	Santa Cruz	Polyclonal	1:50
Anti-dystrophin	Santa Cruz	Polyclonal	1:50
Anti-α-dystroglycan	Millipore	Monoclonal	1:100
Anti-α-sarcoglycan	Leica	Monoclonal	1:100
Anti-laminin-α2	Thermo	Monoclonal	1:100
Anti-connexin43	Sigma	Monoclonal	1:100
Anti-SDHA	Cell Signaling	Polyclonal	1:50

for 5 min at room temperature, then triple-washed with PBS. One drop of anti-fade reagent (Invitrogen) was placed on each slide, and coverslips were applied with the cell surface down. Images of the stained cell samples were acquired with an FV1000D (Olympus, Tokyo, Japan).

Electron Microscopy

Neonatal or iPSC-derived CMs were fixed with 2% glutaraldehyde in 0.1 mmol/L phosphate buffer (pH 7.4) at 4°C for 1 h, washed and immersed overnight in PBS at 4°C, and fixed in 1% buffered osmium tetroxide. Specimens were dehydrated through graded ethanol and embedded in epoxy resin. Ultrathin sections (85 nm) were double-stained with uranyl acetate and lead citrate, and were observed under electron microscopy (H-7600; Hitachi, Tokyo, Japan).

In Vivo Transplantation of iPSC-Derived CMs

For the in vivo transplantation study, 6-old female F344/NJcl-rnu/rnu rats were obtained from Japan Crea (Osaka, Japan) and maintained under specific-pathogen-free conditions in the animal facilities at Osaka University Graduate School of Medicine. A sheet of iPSC-derived CMs was transplanted to the surface of each rat's heart (n=6). Two weeks later, the hearts were excised, quickly frozen in liquid nitrogen-cooled isopentane, sectioned in 6-μm-thick slices in a cryostat, and analyzed by immunofluorescent staining as described before. All animal experiments were approved by the Institutional Animal Care and Use Committee of the Osaka University Graduate School of Medicine before beginning this study.

Stretch- or Growth-Factor-Induced Differentiation of iPSCs to CMs

On day 8, when the iPSC-derived EBs began to differentiate in serum-free medium with insulin-transferin-selenium-X, we tested the effect of growth factor or mechanical stretch stimulation on CM differentiation. We added recombinant IGF1 (20 ng/ml; Abcam, Tokyo, Japan), hepatocyte growth factor (HGF, 10 ng/ml; R&D Systems, Minneapolis, MN, USA) or

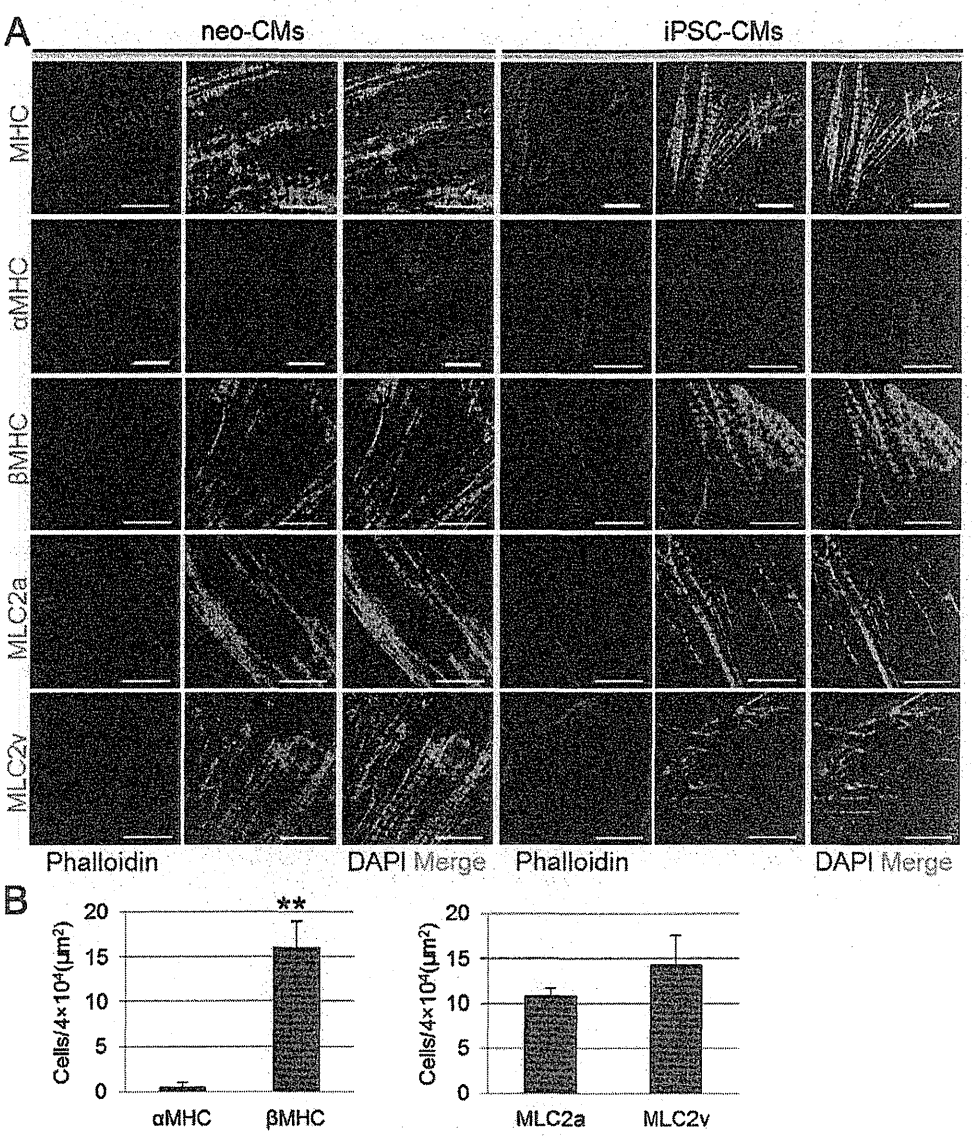

Figure 2. Cytoskeletal proteins in induced pluripotent stem cells (iPSCs). (**A**) Immunofluorescent analysis of cytoskeletal proteins in neonatal cardiomyocytes (neo-CMs) and iPSC-derived CMs (iPSC-CMs). Cells were immunostained with the MHC cytoskeletal proteins, α-MHC (an adult cardiomyocyte marker), β-MHC (a neonatal cardiomyocyte marker), MLC2a, and MLC2v in the sarcomeres (green). Actin was stained with phalloidin. Nuclei were stained with DAPI (blue). Scale bars=10 μm. (**B**) The number of iPSC-CMs expressing α-MHC, β-MHC, MLC2a, or MLC2v. *P<0.05, **P<0.01. MHC, myosin heavy chain; MLC, myosin light chain.

growth hormone (GH, 20 ng/ml; BioVision, Mountain View, CA, USA) to iPSC-derived EBs from day 8 to day 15 to enhance maturity in vitro.

Mechanical stretch was provided by an FX-4000 (Flexcell, Denver, CO, USA) strain unit consisting of a vacuum unit linked to a computer-controlled valve.[28,29] From day 8 to day 15, iPSC-CMs cultured on a flexible membrane base were subjected to cyclic stretch, with a sinusoidal negative pressure peaking at 15 kPa at a frequency of 1 Hz (60 cycles/min) for varying amounts of time. On day 15, iPSC-CMs that had been stimulated by growth factor or mechanical stretch were analyzed for αMHC by immunofluorescent staining.

Statistical Analysis

All data were obtained from at least 3 independent experiments. All values are expressed as the mean±standard deviation. Statistical comparison of the data was performed using unpaired t-tests. A P-value <0.05 was considered statistically significant.

Results

Myocardial Differentiation of Mouse iPSCs In Vitro

In vitro myocardial differentiation of iPSCs was induced using an original protocol established in our laboratory (**Figure 1A**). Serial phenotypic changes in the iPSCs during the differentiation process were analyzed for spontaneous contraction and

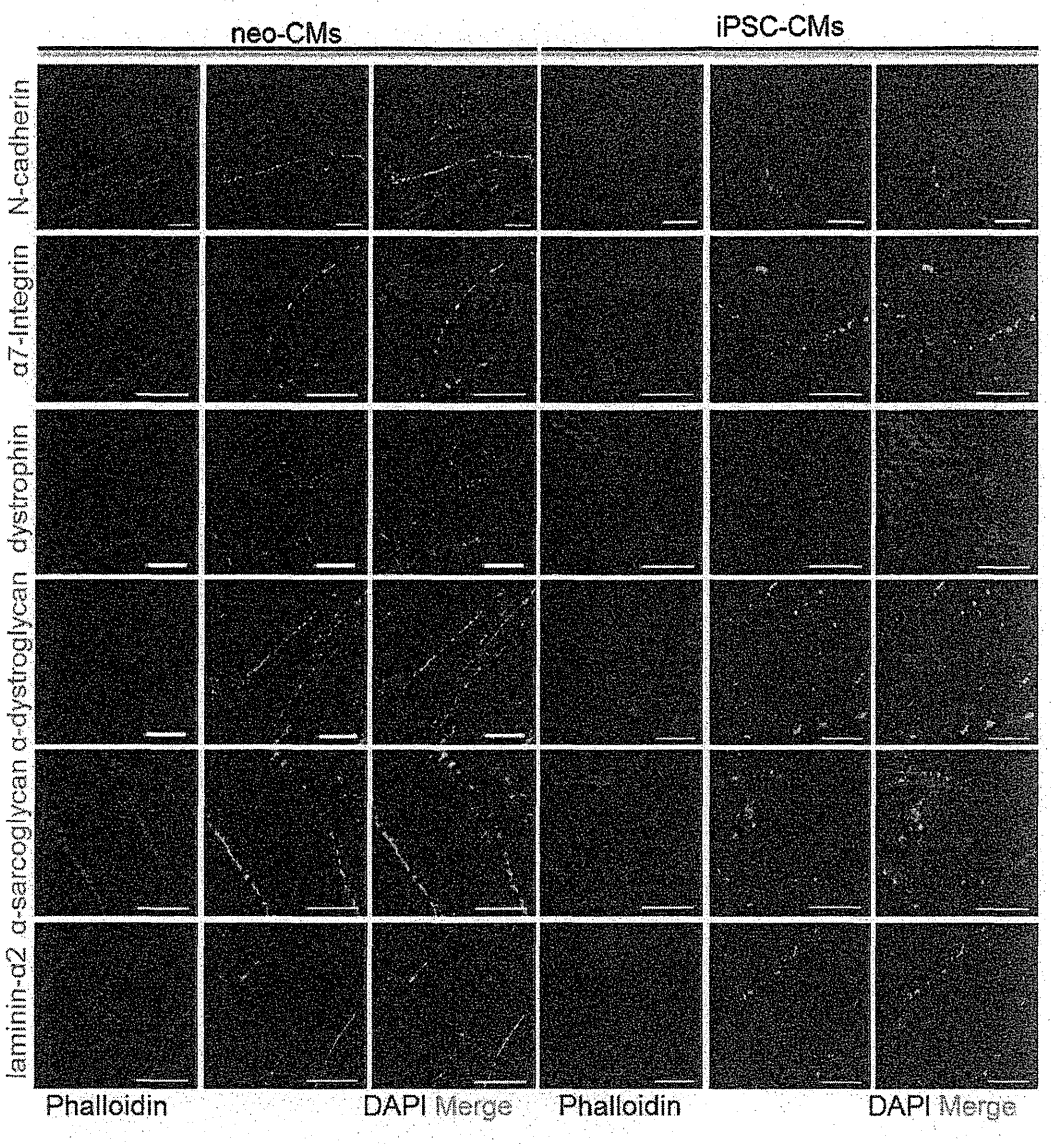

Figure 3. Detection of adhesion molecules in iPSC-derived cardiomyocytes (iPSC-CMs). Immunofluorescent analysis of adhesion molecules in neonatal (neo) CMs and iPSC-CMs. Cells were immunostained for the adhesion molecules N-cadherin, *α*7-integrin, dystrophin, *α*-dystroglycan, *α*-sarcoglycan, and laminin-*α*2 on the cell membrane (green). Actin was stained with phalloidin. Nuclei were stained with DAPI (blue). Scale bars=10 *μ*m. iPSC, induced pluripotent stem cell.

for the expression of cardiac-specific molecules such as GATA4, Nkx2.5, cardiac troponin (cTn) T, myosin light chain (MLC) 2a, sarcomeric *α*-actinin, MHC, connexin43, *α*-sarcoglycan, or N-cadherin. The electrophysiology of terminally differentiated iPSC in vitro was analyzed using a MED 64 system (Panasonic SU-MED640).

From day 10 onwards, some iPSC-derived EBs began to spontaneously contract in a regular, synchronous beating cycle under the culture conditions (**Figure 1B**). The number of contracting EBs gradually increased, reaching a plateau on day 16 (**Figure 1C**). Field-potential recordings of the replated beating colonies, measured by the MED 64 system, showed that the EBs generated regular beats at consistent voltages (**Figure 1D**). RT-PCR showed similar, high expression levels of GATA4, Nkx2.5, and MLC2a on days 6, 8, 12, and 19, while the cTnT expression increased over time (**Figure 1E**). Western blotting revealed that the GATA4, sarcomeric *α*-actinin, MHC, connexin43, *α*-sarcoglycan, and N-cadherin protein levels gradually increased during the differentiation process (**Figure 1F**).

Immunohistochemical Analyses of iPSC-Derived CMs

Immunohistochemical analysis of cytoskeletal and adhesion molecules showed that the expression and distribution of the cardiac-specific protein MHC, the major contractile protein, was similar in iPSC-CMs and neo-CMs (**Figure 2A**). The MHC *α*-isoform, which is the adult CM marker, was rarely expressed by either iPSC-CMs or neo-CMs, but the *β*-isoform, which is the neonatal CM marker, was strongly expressed by both (**Figures 2A,B**). Neo-CMS and iPSC-CMs did not differ in their expression of MLC2a and MLC2v, which are atrial and

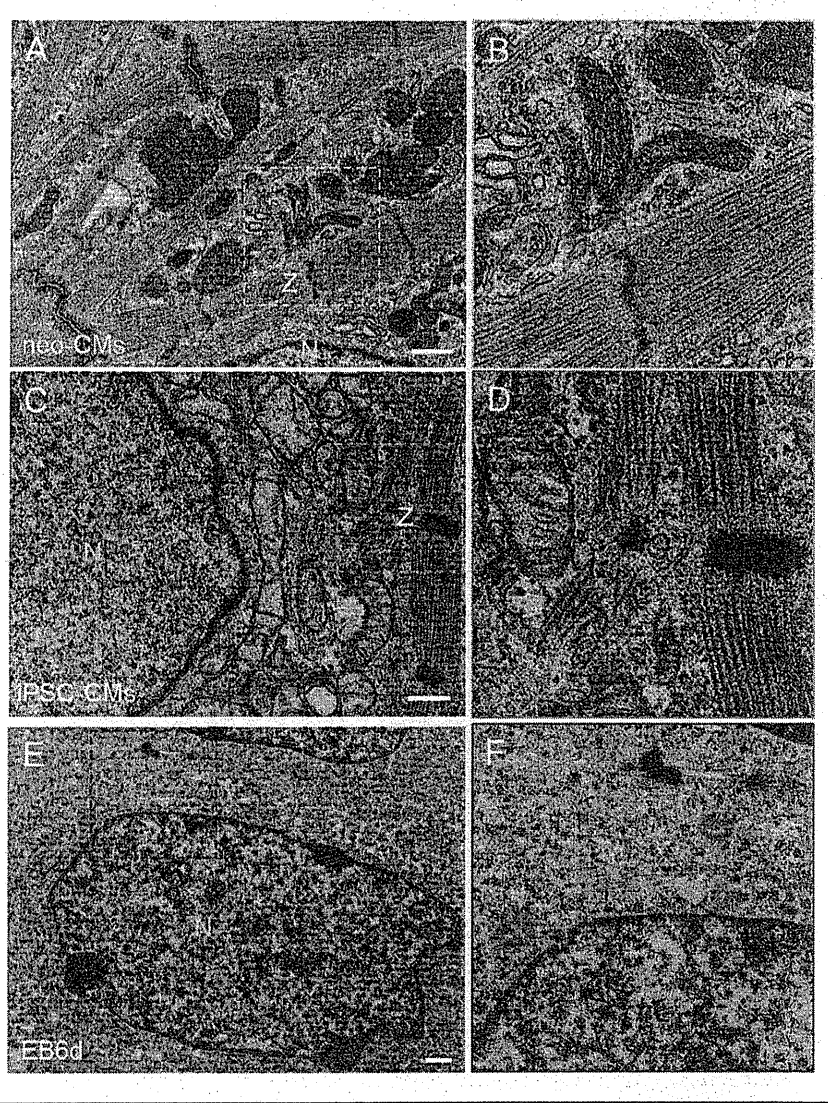

Figure 4. Ultrastructural analysis of iPSC-derived cardiomyocytes (iPSC-CMs). Ultrastructure of neonatal (neo) CMs (**A**,**B**) and iPSC-CMs (beating colonies); (**B**) is a magnified view of (**A**). (**C**,**D**) Embryoid bodies (EBs) on day 6. (**E**,**F**). M: mitochondria, S: sarcomere, Z: Z-bands, N: nucleus. Scale bar=1 μm. iPSC, induced pluripotent stem cell.

ventricular markers, respectively (**Figures 2A,B**). N-cadherin, α7-integrin, α-dystroglycan, α-sarcoglycan, and laminin-α2 were expressed at lower levels on the cell membrane of iPSC-CMs than on the neo-CMs (**Figure 3**). The dystrophin distribution was similar in both types of CM (**Figure 3**).

Ultrastructural Analysis Using Transmission Electron Microscopy In Vitro

We used transmission electron microscopy to compare the neo-CM ultrastructure with that of iPSC-CMs on day 19 and of EBs on day 6. On day 19, the iPSC-CM ultrastructure resembled that of the neo-CM, with abundant myofibrillar bundles with transverse Z-bands and a developed mitochondrial structure. However, there were fewer mitochondria, with lower-density cristae, in the iPSC-CM than in the neo-CM sarcomeric structure. There was no observable sarcomeric structure in the day-6 EBs (**Figure 4**).

Phenotypic Changes in iPSC-Derived CMs Transplanted In Vivo

Cell sheets of iPSC-CMs were transplanted onto adult nude rat hearts. After 2 weeks, we used immunohistochemistry to analyze the expression of cytoskeletal and adhesion molecules in iPSC-CMs compared with fetal or adult murine hearts.

The transplanted iPSC-CMs diffusely expressed and distributed αMHC and βMHC at similar levels, whereas αMHC and βMHC were more predominant in the adult and fetal heart, respectively (**Figure 5A**). Furthermore, αMHC was much more strongly expressed in CMs transplanted in vivo than in CMs cultured in vitro (**Figure 5B,C**). The transplanted iPSC-CMs expressed adhesion molecules such as α-dystroglycan, α-sarcoglycan, and laminin-α2 (**Figure 5B**). DsRed was expressed in iPSC-derived CMs. iPSC-CMs were immunostained with the MHC cytoskeletal proteins (**Figure 5D**).

Effect of Growth Factor or Mechanical Stretch on iPSC Differentiation

We tested the effects of growth factor stimulation and mechanical stretch on iPSC differentiation (**Figure 6A**). Immunofluorescent studies showed that when EBs were stimulated by recombinant IGF-1 for 7 days, the number of contracting EBs increased, and αMHC expression was enhanced (**Figure 6B**). HGF or GH, however, had no effect on the number of contracting EBs or on αMHC expression. Mechanical

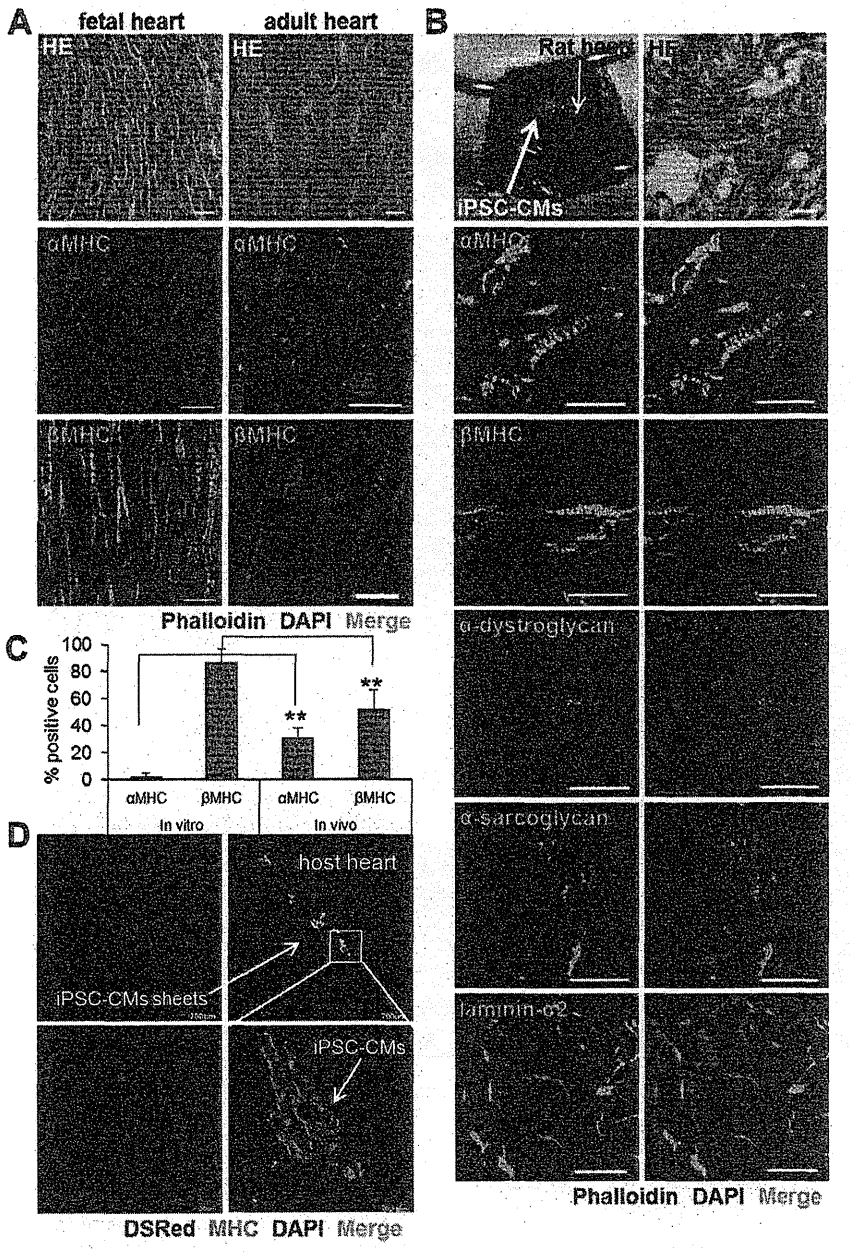

Figure 5. Detection of cytoskeletal and adhesion molecules in transplanted iPSC-derived cardiomyocytes (iPSC-CMs). (**A**) Expression of α-MHC and β-MHC in fetal and adult cardiomyocytes. (**B**) Immunohistochemical analysis of the cytoskeletal and adhesion molecules α-MHC, β-MHC, α-dystroglycan, α-sarcoglycan, and laminin-α2 (green) in transplanted iPSC-CMs. Actin was stained with phalloidin. Nuclei were stained with DAPI (blue). Scale bars=10μm. (**C**) Number of α-MHC-positive cells in cultured iPSC-CMs (in vitro) or transplanted iPSC-CMs (in vivo). (**D**) DsRed was expressed in iPSC-derived CMs. iPSC-CMs were immunostained with the MHC cytoskeletal proteins (green). Nuclei were stained with DAPI (blue). *P<0.05, **P<0.01. iPSC, induced pluripotent stem cell; MHC, myosin heavy chain.

stretch increased the number of beating EBs and elevated the αMHC and SDHA levels in iPSC-CMs (**Figure 6C**). αMHC and SDHA were upregulated in stretch-stimulated iPSC-CMs, whereas connexin43 was downregulated (**Figure 6D**).

Discussion

Although it has been shown that iPSCs can differentiate into CMs in vitro, the ultrastructure and function of iPSC-CMs have not been fully studied.[30] Therefore, we conducted a comprehensive study of the ultrastructure and molecular expression of iPSC-CMs. We found that iPSCs of murine origin differentiated in vitro into CMs with a spontaneous, regular, and synchronous beating cycle. In addition, the differentiated iPSCs exhibited CM-specific markers, such as GATA4, Nkx2.5, cTnT, MLC2a, sarcomeric α-actinin, MHC, connexin43, α-sarcoglycan, and N-cadherin.[31] The expression pattern of the cardiac-specific markers and our ultrastructural findings showed that the morphology and characteristics of iPSC-CMs are similar to those of neo-CMs.

Adhesion molecules, such as α-sarcoglycan or α-dystroglycan, on the cell membrane are important for CM cell-cell and cell-matrix communication, and constitute the CMs functional connections in the myocardium.[32] Although the expression of adhesion molecules in iPSC-CMs is poorly understood, this study clearly showed that iPSC-CMs express these molecules at levels similar to those expressed by neo-CMs. This may indicate that transplanted iPSC-CMs can be efficiently integrated into the myocardium and form functional connections with native CMs and extracellular matrices. In addition, iPSC-CMs expressed laminin-α2, suggesting that an efficient transplantation protocol might induce the formation of adherens

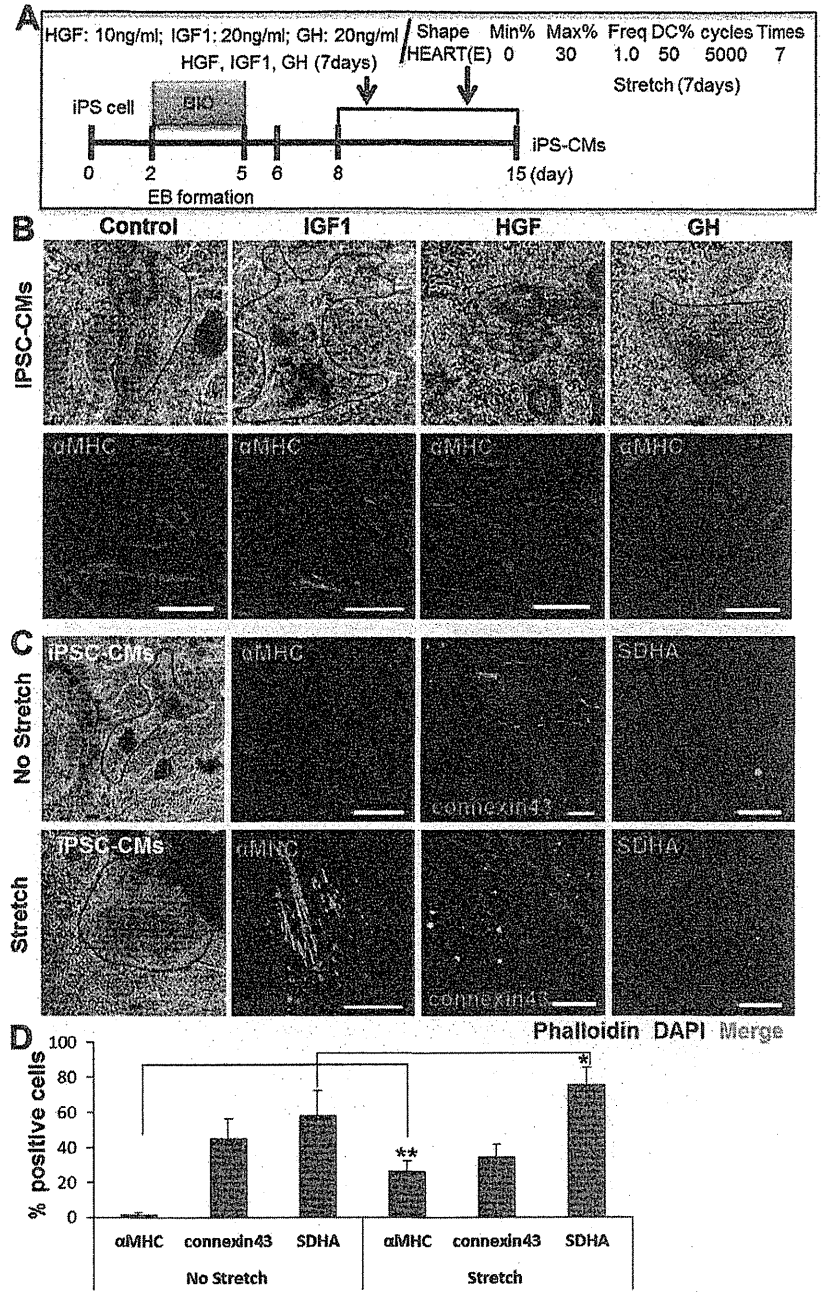

Figure 6. Effects of growth factor or mechanical stretch on differentiation of iPSC-derived cardiomyocytes (iPSC-CMs). (**A**) Protocol for cardiomyocyte differentiation of iPSCs by growth factor stimulation or mechanical stretch in vitro. (**B**) Effects of IGF-1, HGF or GH on the beating areas of EBs (inside red line) and αMHC expression. (**C**) Effects of mechanical stretch on the beating areas of EBs (inside red line), αMHC, connexin43 and SDHA expression. (**D**) αMHC and SDHA were upregulated in stretch-stimulated iPSC-CM, whereas connexin43 was downregulated. Actin stained with phalloidin (red). Nuclei stained with DAPI (blue). Scale bars=10μm. *P<0.05, **P<0.01. EB, embryoid body; GH, growth hormone; HGF, hepatocyte growth factor; IGF-1, insulin-like growth factor-1; iPSC, induced pluripotent stem cell; MHC, myosin heavy chain

junctions with the basement membrane, possibly enhancing the integration of transplanted iPSC-CMs into the heart.

When iPSC-CMs were transplanted into nude rat hearts, they acquired the ability to express α-MHC, an adult CM-specific molecule. Interestingly, stimulation with mechanical stretch or IGF1 enhanced the expression of this marker in iPSC-CMs in vitro.

Mechanical stretch modulates cell alignment and determines cell polarity[16] by altering mechanoreceptor-related gene expression,[33] causing individual CMs to integrate into the functional myocardium. Mechanical stretch has also been shown to induce CMs to secrete or synthesize bioactive molecules such as angiotensin II, IGF-1, tumor necrosis factor α, or vascular endothelial growth factor, which exert both autocrine and paracrine effects on adjacent cells.[34] Thus, mechanical stretch regulates the mechanical and biological functions of both CMs and the myocardium in vivo. These findings suggest that the cardiac environment may be crucial for iPSC-CMs to fully mature.

Our ultrastructural analysis showed that the sarcomeric structure and the mitochondrial quantity, function, and structure were less developed in the iPSC-CMs than in neo-CMs. However, transplanting iPSC-CMs into the heart induced a transition from the β to the α MHC isoform, a transition seen during cardiac development and maturation.[35] Although this study did not investigate changes in mitochondrial quantity or structure in iPSC-CMs after transplantation into the heart, the maturing of MHC after transplantation implies a functional im-

provement of the mitochondria.

Transplantation of iPSC-CMs is a promising method for regenerating or replacing lost or damaged myocardial tissues in situ, although the optimal transplantation method is still under debate.[36] The cell-sheet method used in this study has been shown to preserve the functionality, and thus the quantity, of cells transplanted into the heart, with minimal damage.[32] This study also showed that further differentiation was induced in situ in iPSC-CMs transplanted by the cell-sheet method, although the contribution of these cells to regional or global cardiac function was not studied. These findings warrant further functional, electrophysiological, and biological studies to optimize the transplantation protocol of iPSC-CMs for the greatest therapeutic effect against cardiac failure.

In conclusion, iPSCs of murine origin were not only efficiently differentiated in vitro into CMs with a phenotype and function like that of neo-CMs, but could also be differentiated to express adult CM-specific molecules. This differentiation process might be promoted in vitro by IGF-1 stimulation or mechanical stretch. These results suggest iPSC-CMs could be a useful source for cell therapy for the future treatment of heart failure.

Acknowledgments

This work was supported by the Highway Program for Realization of Regenerative Medicine from the Japanese Ministry of Education, Culture, Sports, Science and Technology.

References

1. Towbin JA, Bowles NE. The failing heart. *Nature* 2002; **415:** 227–233.
2. Hosseinkhani M, Hasegawa K, Ono K, Kawamura T, Takaya T, Morimoto T, et al. Trichostatin A induces myocardial differentiation of monkey ES cells. *Biochem Biophys Res Commun* 2007; **356:** 386–391.
3. Dimmeler S, Zeiher AM, Schneider MD. Unchain my heart: The scientific foundations of cardiac repair. *J Clin Invest* 2005; **115:** 572–583.
4. Dinsmore J, Ratliff J, Deacon T, Pakzaban P, Jacoby D, Galpern W, et al. Embryonic stem cells differentiated in vitro as a novel source of cells for transplantation. *Cell Transplant* 1996; **5:** 131–143.
5. Segers VF, Lee RT. Stem-cell therapy for cardiac disease. *Nature* 2008; **451:** 937–942.
6. Fukuda K. Progress in myocardial regeneration and cell transplantation. *Circ J* 2005; **69:** 1431–1446.
7. Uemura R, Xu M, Ahmad N, Ashraf M. Bone marrow stem cells prevent left ventricular remodeling of ischemic heart through paracrine signaling. *Circ Res* 2006; **98:** 1414–1421.
8. Choi SH, Jung SY, Kwon SM, Baek SH. Perspectives on stem cell therapy for cardiac regeneration. *Circ J* 2012; **76:** 1307–1312.
9. Perino MG, Yamanaka S, Li J, Wobus AM, Boheler KR. Cardiomyogenic stem and progenitor cell plasticity and the dissection of cardiopoiesis. *J Mol Cell Cardiol* 2008; **45:** 475–494.
10. Yuasa S, Fukuda K. Cardiac regenerative medicine. *Circ J* 2008; **72:** 49–55.
11. Chen H, Hattori F, Murata M, Li W, Yuasa S, Onizuka T, et al. Common marmoset embryonic stem cell can differentiate into cardiomyocytes. *Biochem Biophys Res Commun* 2008; **369:** 801–806.
12. Iwamuro M, Komaki T, Kubota Y, Seita M, Kawamoto H, Yuasa T, et al. Comparative analysis of endoderm formation efficiency between mouse ES cells and iPS cells. *Cell Transplant* 2010; **19:** 831–839.
13. Mandai M, Ikeda H, Jin ZB, Iseki K, Ishigami C, Takahashi M. Use of lectins to enrich mouse ES-derived retinal progenitor cells for the purpose of transplantation therapy. *Cell Transplant* 2010; **19:** 9–19.
14. Li X, Yu X, Lin Q, Deng C, Shan Z, Yang M, et al. Bone marrow mesenchymal stem cells differentiate into functional cardiac phenotypes by cardiac microenvironment. *J Mol Cell Cardiol* 2007; **42:** 295–303.
15. Reinecke H, Minami E, Zhu WZ, Laflamme MA. Cardiogenic differentiation and transdifferentiation of progenitor cells. *Circ Res* 2008; **103:** 1058–1071.
16. Matsuda T, Takahashi K, Nariai T, Ito T, Takatani T, Fujio Y, et al. N-cadherin-mediated cell adhesion determines the plasticity for cell alignment in response to mechanical stretch in cultured cardiomyocytes. *Biochem Biophys Res Commun* 2005; **326:** 228–232.
17. Sadoshima J, Jahn L, Takahashi T, Kulik TJ, Izumo S. Molecular characterization of the stretch-induced adaptation of cultured cardiac cells: An in vitro model of load-induced cardiac hypertrophy. *J Biol Chem* 1992; **267:** 10551–10560.
18. Komuro I, Kaida T, Shibazaki Y, Kurabayashi M, Katoh Y, Hoh E, et al. Stretching cardiac myocytes stimulates protooncogene expression. *J Biol Chem* 1990; **65:** 3595–3598.
19. Ruwhof C, van der Laarse A. Mechanical stress-induced cardiac hypertrophy: Mechanisms and signal transduction pathways. *Cardiovasc Res* 2000; **7:** 23–37.
20. Shyu KG. Cellular and molecular effects of mechanical stretch on vascular cells and cardiac myocytes. *Clin Sci Lond* 2009; **16:** 377–389.
21. Shyu KG, Ko WH, Yang WS, Wang BW, Kuan P. Insulin-like growth factor-1 mediates stretch-induced upregulation of myostatin expression in neonatal rat cardiomyocytes. *Cardiovasc Res* 2005; **68:** 405–414.
22. Eschenhagen T, Didié M, Heubach J, Ravens U, Zimmermann WH. Cardiac tissue engineering. *Transpl Immunol* 2002; **9:** 315–321.
23. Okita K, Ichisaka T, Yamanaka S. Generation of germline-competent induced pluripotent stem cells. *Nature* 2007; **48:** 313–317.
24. Nakagawa M, Koyanagi M, Tanabe K, Takahashi K, Ichisaka T, Aoi T, et al. Generation of induced pluripotent stem cells without Myc from mouse and human fibroblasts. *Nat Biotechnol* 2008; **26:** 101–106.
25. Naito AT, Shiojima I, Akazawa H, Hidaka K, Morisaki T, Kikuchi A, et al. Developmental stage-specific biphasic roles of Wnt/beta-catenin signaling in cardiomyogenesis and hematopoiesis. *Proc Natl Acad Sci USA* 2006; **103:** 19812–19817.
26. Zhang CM, Gao L, Zheng YJ, Yang HT. Berbamine protects the heart from ischemia/reperfusion injury by maintaining cytosolic Ca^{2+} homeostasis and preventing calpain activation. *Circ J* 2012; **76:** 1993–2002.
27. Miyagawa S, Saito A, Sakaguchi T, Yoshikawa Y, Yamauchi T, Imanishi Y, et al. Impaired myocardium regeneration with skeletal cell sheets--a preclinical trial for tissue-engineered regeneration therapy. *Transplantation* 2010; **90:** 364–372.
28. Shyu KG, Chen CC, Wang BW, Kuan PL. Angiotensin II receptor antagonist blocks the expression of connexin43 induced by cyclical mechanical stretch in cultured neonatal rat cardiac myocytes. *J Mol Cell Cardiol* 2001; **3:** 691–698.
29. Chang H, Wang BW, Kuan P, Shyu KG. Cyclical mechanical stretch enhances angiopoietin-2 and Tie2 receptor expression in cultured human umbilical vein endothelial cells. *Clin Sci* 2003; **104:** 421–428.
30. Rajala K, Pekkanen-Mattila M, Aalto-Setälä K. Cardiac differentiation of pluripotent stem cells. *Stem Cells Int* 2011; **2011:** 4061–4073.
31. Gao XR, Tan YZ, Wang HJ. Overexpression of Csx/Nkx2.5 and GATA-4 enhances the efficacy of mesenchymal stem cell transplantation after myocardial infarction. *Circ J* 2011; **75:** 2683–2691.
32. Ozawa E, Mizuno Y, Hagiwara Y, Sasaoka T, Yoshida M. Molecular and cell biology of the sarcoglycan complex. *Muscle Nerve* 2005; **2:** 563–576.
33. Aikawa R, Nagai T, Kudoh S, Zou Y, Tanaka M, Tamura M, et al. Integrins play a critical role in mechanical stress-induced p38 MAPK activation. *Hypertension* 2002; **9:** 233–238.
34. Sadoshima J, Xu Y, Slayter HS, Izumo S. Autocrine release of angiotensin II mediates stretch-induced hypertrophy of cardiac myocytes in vitro. *Cell* 1993; **75:** 977–984.
35. Nishi H, Ono K, Horie T, Nagao K, Kinoshita M, Kuwabara Y, et al. MicroRNA-27a regulates beta cardiac myosin heavy chain gene expression by targeting thyroid hormone receptor beta1 in neonatal rat ventricular myocytes. *Mol Cell Biol* 2011; **31:** 744–755.
36. Gonzales C, Pedrazzini T. Progenitor cell therapy for heart disease. *Exp Cell Res* 2009; **315:** 3077–3085.

Enhanced Survival of Transplanted Human Induced Pluripotent Stem Cell–Derived Cardiomyocytes by the Combination of Cell Sheets With the Pedicled Omental Flap Technique in a Porcine Heart

Masashi Kawamura, MD; Shigeru Miyagawa, MD, PhD; Satsuki Fukushima, MD, PhD; Atsuhiro Saito, PhD; Kenji Miki, PhD; Emiko Ito, PhD; Nagako Sougawa, PhD; Takuji Kawamura, MD; Takashi Daimon, PhD; Tatsuya Shimizu, MD, PhD; Teruo Okano, PhD; Koichi Toda, MD, PhD; Yoshiki Sawa, MD, PhD

Background—Transplantation of cardiomyocytes that are derived from human induced pluripotent stem cell–derived cardiomyocytes (hiPS-CMs) shows promise in generating new functional myocardium in situ, whereas the survival and functionality of the transplanted cells are critical in considering this therapeutic impact. Cell-sheet method has been used to transplant many functional cells; however, potential ischemia might limit cell survival. The omentum, which is known to have rich vasculature, is expected to be a source of blood supply. We hypothesized that transplantation of hiPS-CM cell sheets combined with an omentum flap may deliver a large number of functional hiPS-CMs with enhanced blood supply.

Methods and Results—Retrovirally established human iPS cells were treated with Wnt signaling molecules to induce cardiomyogenic differentiation, followed by superparamagnetic iron oxide labeling. Cell sheets were created from the magnetically labeled hiPS-CMs using temperature-responsive dishes and transplanted to porcine hearts with or without the omentum flap (n=8 each). Two months after transplantation, the survival of superparamagnetic iron oxide–labeled hiPS-CMs, assessed by MRI, was significantly greater in mini-pigs with the omentum than in those without it; histologically, vascular density in the transplanted area was significantly greater in mini-pigs with the omentum than in those without it. The transplanted tissues contained abundant cardiac troponin T–positive cells surrounded by vascular-rich structures.

Conclusions—The omentum flap enhanced the survival of hiPS-CMs after transplantation via increased angiogenesis, suggesting that this strategy is useful in clinical settings. The combination of hiPS-CMs and the omentum flap may be a promising technique for the development of tissue-engineered vascular-rich new myocardium in vivo. (***Circulation.*** **2013;128[suppl 1]:S87-S94.)**

Key Words: cell transplantation ■ induced pluripotent stem cells ■ regeneration

Stem cell therapy shows promise in the treatment of heart failure. However, the therapeutic benefits proven by clinical studies in the past decade were only modest, indicating that further investigations and refinements are required to establish this treatment in the clinical arena.[1,2] The success of cell transplantation therapy for heart failure is dependent on the choice of cell source, cell delivery method, and target cardiac pathology. In these previous clinical trials, transplantation of somatic tissue–derived stem or progenitor cells has shown no or low cardiomyogenic differentiation capacity in vivo, but contributed to functional recovery via paracrine effects, potentially limiting the therapeutic effects, in particular, in treating severe heart failure.[1–4] In addition, it has been shown that direct intramyocardial or intracoronary injection of dissociated single cells, which was used in most of the clinical studies, yields <10% of engraftment rate of the cells immediately after transplantation, indicating that further refinement of the cell delivery method would be required to increase cell engraftment and enhance the consequent therapeutic effects.[1,2]

Human induced pluripotent stem (hiPS) cells are initially established by nuclear reprogramming of somatic cells.[5,6] hiPS cell carries a capacity of unlimited proliferation and differentiation to cardiomyocyte.[7] Transplantation of hiPS-derived cardiomyocytes (hiPS-CMs) would have, thus, a potential to

From the Department of Cardiovascular Surgery, Osaka University Graduate School of Medicine, Suita, Osaka, Japan (M.K., S.M., S.F., K.M., E.I., N.S., T.K., K.T., Y.S.); Medical Center for Translational Research, Osaka University Hospital, Suita, Osaka, Japan (A.S.); Department of Biostatistics, Hyogo College of Medicine, Nishinomiya, Hyogo, Japan (T.D.); Institute of Advanced Biomedical Engineering and Science, Tokyo Women's Medical University, Tokyo, Japan (T.S., T.O.).

Presented at the 2012 American Heart Association meeting in Los Angeles, CA, November 3–7, 2012.

The online-only Data Supplement is available with this article at http://circ.ahajournals.org/lookup/suppl/doi:10.1161/CIRCULATIONAHA.112.000366/-/DC1.

Correspondence to Yoshiki Sawa, MD, PhD, Department of Cardiovascular Surgery, Osaka University Graduate School of Medicine, 2-2(E1) Yamadaoka, Suita, Osaka 565-0871, Japan. E-mail sawa-p@surg1.med.osaka-u.ac.jp

Circulation **is available at http://circ.ahajournals.org** **DOI: 10.1161/CIRCULATIONAHA.112.000366**

increase the functional cardiomyocytes in damaged heart tissue to mechanically contribute to cardiac function. In addition, the recently developed scaffoldless tissue engineering technique of cell-sheet engineering is applicable to myocardial regeneration therapy.[8] This technique preserves extracellular matrix without artificial scaffolds, which may prevent cell detachment–associated anoikis.[9] In contrast to the needle injection technique, the cell-sheet technique can deliver a large number of cells to the damaged myocardium without loss of transplanted cells or injury to the host myocardium.[10,11] Importantly, this method has already shown feasibility and safety in the clinical study.[12] On these bases, we studied the therapeutic efficacy of transplantation of hiPS-CMs with the cell-sheet method in a porcine chronic ischemic cardiomyopathy model.[13] This study, however, showed that the transplanted cells rarely survived in the heart long-term, possibly because of poor vascular network support from the native tissue.

The omentum has been historically used in surgical revascularization for patients with ischemic heart disease[14–16] and is also known to have rich vasculature and angiogenic factors.[17,18] Importantly, we reported that a pedicle omentum flap covering the transplanted skeletal myoblast cell sheets enhanced angiogenesis over the cell-sheet–transplanted territory, survival of cells, and therapeutic effects.[19] We herein hypothesized that covering with an omentum flap may enhance the survival of transplanted hiPS-CM cell sheets via the promotion of angiogenesis over the transplanted territory. In this study, we compared the survival of hiPS-CMs, with or without a pedicle omentum flap, after transplantation to the mini-pig heart, and we examined whether the omentum enhanced the angiogenic capacity of hiPS-CM sheets in vivo.

Materials and Methods

All experimental procedures were approved by the institutional ethics committee. Animal care was conducted humanely in compliance with the Principles of Laboratory Animal Care formulated by the National Society for Medical Research and the Guide for the Care and Use of Laboratory Animals prepared by the Institute of Animal Resources and published by the National Institutes of Health (publication no. 85-23, revised 1996).

Preparation of SPIO-Labeled hiPS-CM Cell Sheets

The hiPS cell line 201B7 that was generated using the 4 transcription factors Oct4, Sox2, Klf4, and c-Myc was used in this study.[5] Culture of the hiPS cells, formation of the embryoid bodies, and subsequent cardiomyogenic differentiation and purification were performed as described previously to generate hiPS-CMs.[13] The purified hiPS-CMs were then labeled with the superparamagnetic iron oxide (SPIO) ferucarbotran (Resovist; Bayer Pharma, Berlin, Germany) using the hemagglutinating virus of Japan envelope vector (GenomOne-Neo; Ishihara Sangyo, Osaka, Japan).[20,21] Subsequently, human mesenchymal stem cells (Lonza, Basel, Switzerland) were seeded at a density of 5×10^6 cells/dish onto 10-cm UpCell dishes, on which the SPIO-labeled hiPS-CMs were grown. The next day, the dishes were incubated at room temperature, which induced the cells to detach spontaneously to form scaffold-free hiPS-CM cell sheets.

Flow Cytometry

Dissociated cells after hiPS cell differentiation were fixed, permeabilized, and labeled with anticardiac isoform of troponin T (cTNT; clone 13211; Thermo Fisher scientific, Runcorn, UK) conjugated with Alexa-488 using Zenon technology (Invitrogen), followed by analysis on BD FACSCanto II (BD Biosciences) with BD FACSDiva Software (BD Biosciences).

Study Protocol

Normal 16 female mini-pigs (Japan Farm Co Ltd, Kagoshima, Japan) weighing 20 to 25 kg were randomly divided into 2 groups (n=8 each) to perform hiPS-CM cell-sheet transplantation either with or without the pedicle omentum translocation. All animals were immunosuppressed by daily administration of tacrolimus (0.75 mg/kg; Astellas, Tokyo, Japan), mycophenolate mofetil (500 mg; Teva Czech Industries s.r.o, Opava, Czech), and prednisolone (20 mg; Takeda Pharmaceutical Co Ltd, Osaka, Japan) daily from 5 days before transplantation until euthanasia. Cardiac MRI scans were taken on the same mini-pigs at 1 week, 4 weeks, and 8 weeks after transplantation. After the final scan, the mini-pigs were humanely euthanized for analysis (Figure 1A).

Transplantation of SPIO-Labeled hiPS-CM Cell Sheets Covered With the Pedicle Omentum

All animals were preanesthetized with ketamine hydrochloride (20 mg/kg; Daiichi Sankyo, Tokyo, Japan) and xylazine (2 mg/kg; Bayer HealthCare, Leverkusen, Germany), intubated endotracheally, and maintained by continuous infusion of propofol (6 mg/kg per hour; AstraZeneca K.K., Osaka, Japan) and vecuronium bromide (0.05 mg/kg per hour; Daiichi Sankyo). Seven SPIO-labeled hiPS-CM sheets were placed on the epicardium via the median sternotomy. In the case of transplantation of the cell sheet covered with the pedicled omentum, the omentum was mobilized to the mediastinal space via additional small upper midline laparotomy, preserving both gastroepiploic arteries and their arcade. Initially, 4 hiPS-CM cell sheets were placed on the epicardium and covered with the omentum. The remaining 3 hiPS-CM cell sheets, then, were placed on the covering omentum and covered with the omentum again (Figure 1B). The omentum was stitched and fixed on the excised pericardium (Figure 1C). Mini-pigs were then allowed to recover and were later humanely euthanized.

Cardiac MRI

ECG-gated cardiac MRI (CMR) was performed under general anesthesia with an 8-channel cardiac coil wrapped around the chest wall.[22] CMR images were acquired on a 1.5-T MR scanner (Signa EXCITE XI TwinSpeed; GE Medical Systems, Milwaukee, WI). To assess SPIO-labeled hiPS-CM detection, animals were imaged 1 week after transplantation. In addition, 1 animal was reimaged at 4 and 8 weeks after transplantation to detect SPIO-labeled hiPS-CM retention. Short-axis images with 8-mm slice thickness, including the entire heart, were obtained by pulse parameters for cardiac-gated, fast gradient–recalled echo. The SPIO-labeled hiPS-CM hypointense area was measured using planimetry of fast gradient–recalled echo images on a workstation (Virtual Place Lexus64; AZE, Tokyo, Japan). The survival proportion of hiPS-CMs was determined using the hypointense area at 4 and 8 weeks after transplantation divided by the area at 1 week after transplantation as the baseline.

Histology and Immunohistolabeling

The hiPS-CM cell sheets and the excised heart specimens were either embedded in paraffin or optimal cutting temperature compound (Tissueb Tek; Sakura Finetek, Torrance, CA) for frozen section. The paraffin-embedded sections were stained with hematoxylin–eosin or Prussian blue that visualizes iron contents. Ten different fields were randomly selected. The number of spindle-shaped cells with a nucleus and iron in the cytoplasm in each field was counted with a light microscopy under high-power magnification (×400). Cells from 10 fields were averaged, and the results are expressed as cell density (per high-power field). In addition, the paraffin-embedded sections were immunolabeled with anti-human von Willebrand factor antibody (Dako, Glostrup, Denmark) and visualized with the horseradish peroxidase-based EnVision kit (Dako). Ten different fields were randomly selected, and the number of von Willebrand factor–positive

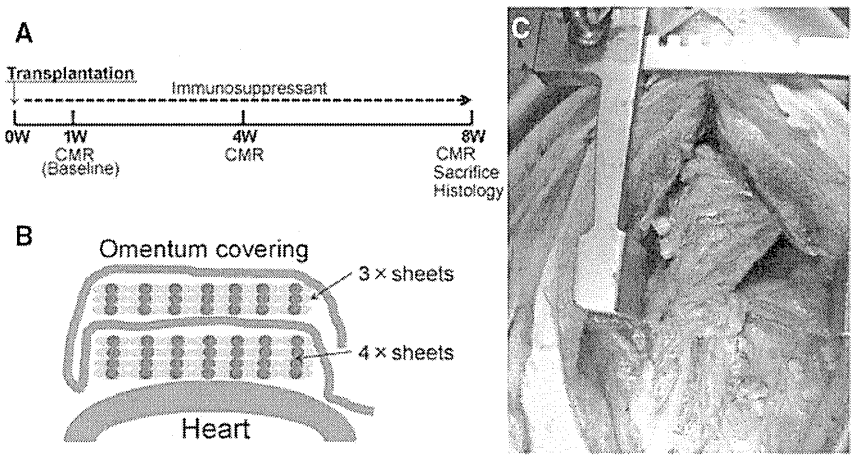

Figure 1. Study protocol of the mini-pig experiment and operative procedure. **A**, Schedule of cardiac MRI (CMR) and histological evaluations. **B**, Procedural scheme of cell-sheet transplantation with the omentum. **C**, Image taken after treatment. The omentum is mobilized and transplanted with the cell sheets on the heart through median sternotomy with an additional upper midline laparotomy.

cells in each field was counted using a light microscope under high-power magnification (×200). The stained blood vessels from the 10 fields were averaged and the results expressed as vascular density (per square millimeter). The frozen sections were immunolabeled with anti-cTNT antibody (1:100 dilution; Abcam, Cambridge, UK) and anti-CD68 antibody for macrophages (1:100 dilution, Abcam) as primary antibodies and visualized with AlexaFluor488–conjugated goat anti-mouse (Invitrogen) and AlexaFluor555–conjugated goat anti-rabbit (Invitrogen) as secondary antibodies. Nuclei were counterstained with 4′,6-diamidino-2-phenylindole (Dojindo, Tokyo, Japan) and assessed using the Biorevo BZ-9000 (Keyence) or confocal microscopy (Olympus Japan, FV1000-D IX81, Tokyo, Japan). SPIO particles of Prussian blue staining were visualized by differential interference contrast of confocal microscopy.

Real-Time Polymerase Chain Reaction

Total RNA was extracted from cardiac tissue and reverse transcribed using Omniscript reverse transcriptase (Qiagen, Hilden, Germany) with random primers (Invitrogen), and the resulting cDNA was used for real-time polymerase chain reaction with the ABI PRISM 7700 (Applied Biosystems, Stockholm, Sweden) system using pig-specific primers (Applied Biosystems) for vascular endothelial growth factor (VEGF), basic fibroblast growth factor, and stromal-derived factor-1 (SDF-1). Each sample was analyzed in triplicate for each gene studied. Data were normalized to GAPDH expression level. For relative expression analysis, the delta-delta Ct method was used, and values of the cell-sheet transplantation without the omentum were used as reference values.

Statistical Analysis

Data are expressed as means±SDs. Comparisons between 2 groups were made using Welch t test. Cell survival proportion over time was assessed by repeated-measures ANOVA with group, time, and group×time interaction effects. All P values are 2-sided, and values of $P<0.05$ were considered to indicate statistical significance. Statistical analyses were performed using JMP 9.02 (SAS Institute, Cary, NC).

Results

Generation of SPIO-Labeled hiPS-CM Cell Sheets

Cardiomyogenic differentiation of hiPS cells was induced by treatment of the embryoid bodies formed from cultured hiPS cells with Wnt3a and R-spondin-1. Subsequently, the differentiated hiPS cells were purified by culture in glucose-free medium to yield ≈1 to 2×10^7 hiPS-CMs. Approximately 80% (83.6±8.1%) of the hiPS-CMs were positive for cTNT, as determined by flow cytometry (Figure 2A). After SPIO labeling to the hiPS-CMs, human mesenchymal stem cells were added to the hiPS-CM culture. Subsequently, culture in the thermoresponsive dishes yielded round-shaped hiPS-CM cell sheets (Figure 2B). The hiPS-CMs on the sheet continued to beat before and after detaching from culture surface (Movies I and II in the online-only Data Supplement). Immunohistolabeling showed that the large number of cells in the hiPS-CM cell sheets were homogeneously positive for cTNT (Figure 2C). Prussian blue staining confirmed that the hiPS-CMs contained iron in the cytoplasm (Figure 2D).

In Vivo Analysis of Survival of Transplanted SPIO-Labeled hiPS-CMs by Serial CMR

Transplantation of the same number of hiPS-CM cell sheets with or without the omentum covering was successfully performed via median sternotomy in 16 normal mini-pigs. There was no mortality related to the procedure or otherwise before the planned euthanasia. In addition, the omentum was attached to the surface of the heart in all mini-pigs with the omentum. CMRs were performed to assess the survival of transplanted SPIO-labeled hiPS-CMs at 1 week (baseline), 4 weeks, and 8 weeks after cell transplantation.

SPIO signals were clearly identified as the hypointense area in the surface of the left ventricle by CMR in all mini-pigs throughout the study period (Figure 3A). SPIO-positive hypointense area was gradually decreased in both the groups during the 8 weeks, whereas the SPIO-positive area was larger and thicker in mini-pigs with the omentum compared with those without the omentum during the study period. The survival proportion of the SPIO-labeled hiPS-CMs was determined by the formula that the hypointense area at 4 and 8 weeks after transplantation was divided by the area at 1 week after transplantation as baseline. Both groups showed steady decrease in the cell survival during the 7 weeks, whereas the proportion of decrease was significantly less in mini-pigs with the omentum than in those without it at 4 weeks (92±10% versus 60±10%) and 8 weeks (78±10% versus 42±9%) after treatment ($P<0.0001$ for interaction effect of time and group in the repeated ANOVA; Figure 3B).

Histological Evaluation of Transplanted hiPS-CMs With or Without the Omentum

Excised heart tissues at 8 weeks after transplantation were assessed by histology. The transplanted hiPS-CMs and the

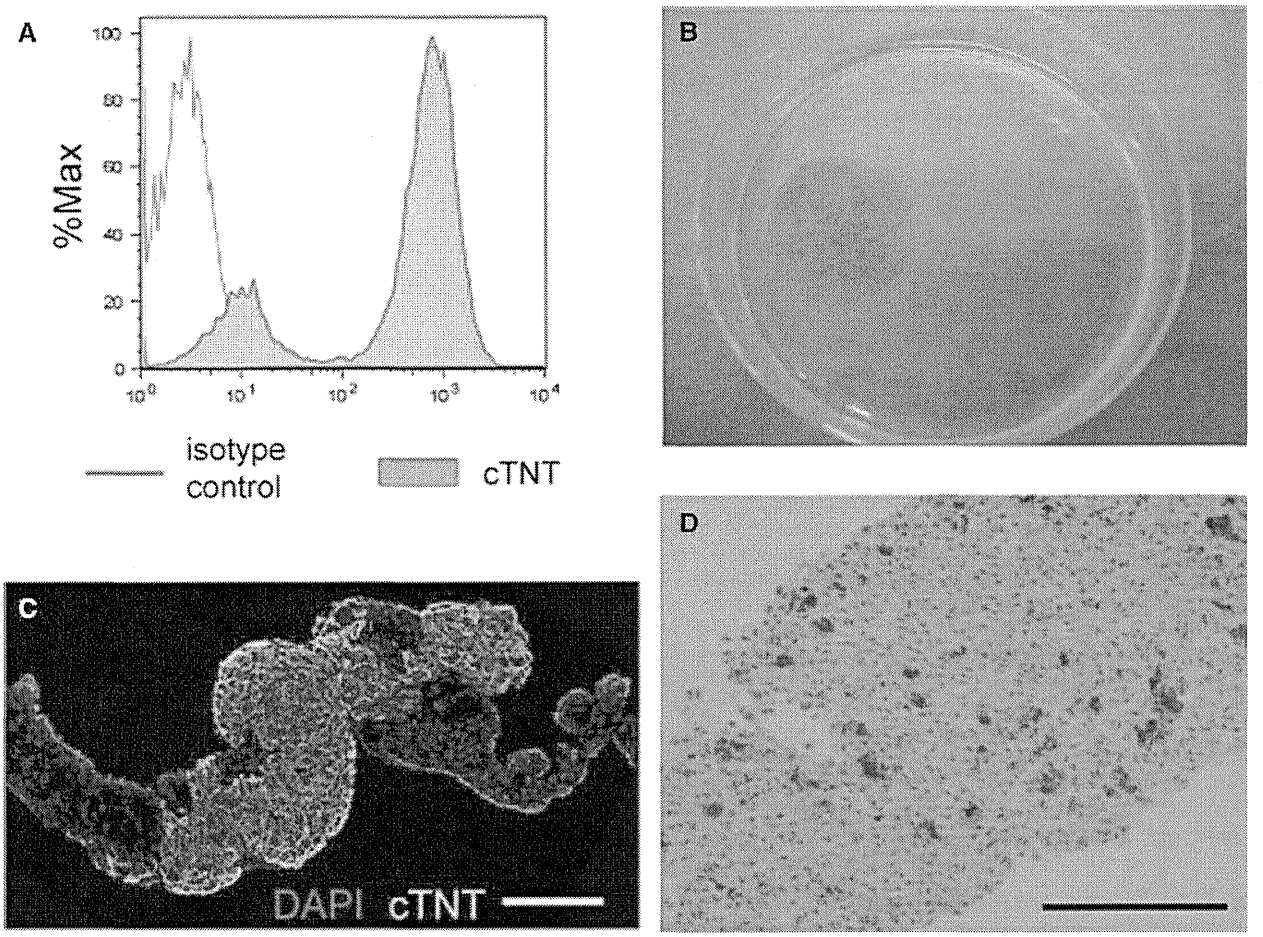

Figure 2. Histological characteristics of the human induced pluripotent stem cell–derived cardiomyocyte (hiPS-CM) cell sheet. **A**, Expression of cardiac troponin T (cTNT) after differentiation and purification of hiPS-CMs. **B**, A superparamagnetic iron oxide (SPIO)–labeled hiPS-CM cell sheet in a 10-cm dish. **C**, Immunostaining of the hiPS-CM cell sheet with cTNT antibody (green). The cell nuclei were counterstained with 4′,6-diamidino-2-phenylindole (DAPI; blue). **D**, Prussian blue staining of the SPIO-labeled hiPS-CM cell sheet. Scale bar, 50 μm in **C** and **D**.

pedicle omentum were attached over the epicardium of the left ventricle without any histological gaps in all mini-pigs, as assessed by hematoxylin–eosin staining (Figure 4D). The hearts without the omentum showed cellular and fibrous components over the anterior wall of the ventricles (Figure 4A), whereas the hearts with the omentum showed thick cellular, fibrous, and fat-rich components covering the anterior and lateral wall of the ventricles (Figure 4D).

Prussian blue staining revealed cells containing iron on the surface of the ventricles, corresponding to the area seen on CMR in both groups (Figure 4B and 4E). A larger number of cells with iron contents were identified in mini-pigs with the omentum compared with those without (Figure 4B, 4C, 4E, and 4F). In fact, the density of iron-containing cells in the transplanted site, assessed semiquantitatively by Prussian blue staining at 8 weeks after treatment, was significantly greater in the mini-pig with the omentum (27±6 cells/high-power field) than in those without it (5±2 cells/high-power field; $P<0.0001$; Figure 4G). Immunohistolabeling showed that a larger number of cells are positive for cTNT in the area where cells with iron inclusions are present in mini-pigs with the omentum compared with those without it (Figure 4H). The distribution of the SPIO particles was visualized by differential interference contrast of confocal microscopy. Grafted hiPS-CMs were identified and confirmed as double-positive for cTNT and SPIO and negative for CD68, which is a specific marker for macrophages, by immunohistolabeling (Figure 4I–4N). In addition, no teratomas were formed in the heart or other thoracic organs at 8 weeks after the transplantation of the hiPS-CM cell sheets with or without the omentum (data not shown).

Capillary Density in the Transplanted Area

Vessels and capillaries in the transplanted cell sheets at 8 weeks after transplantation were visualized and assessed by immunohistochemistry for von Willebrand factor. The transplanted cell sheets without the omentum contained a large number of capillaries and a small number of vessels in a homogeneous manner (Figure 5A), suggesting that vascular network was created possibly to support the survival and function of the cell sheets. Of note, the number of capillaries and vessels were markedly greater in the cell sheets covered by the omentum compared with those without it (Figure 5B). In fact, capillary density in the transplanted cell sheets, assessed semiquantitatively by immunohistochemistry for von Willebrand factor at 8 weeks after treatment, was significantly and markedly

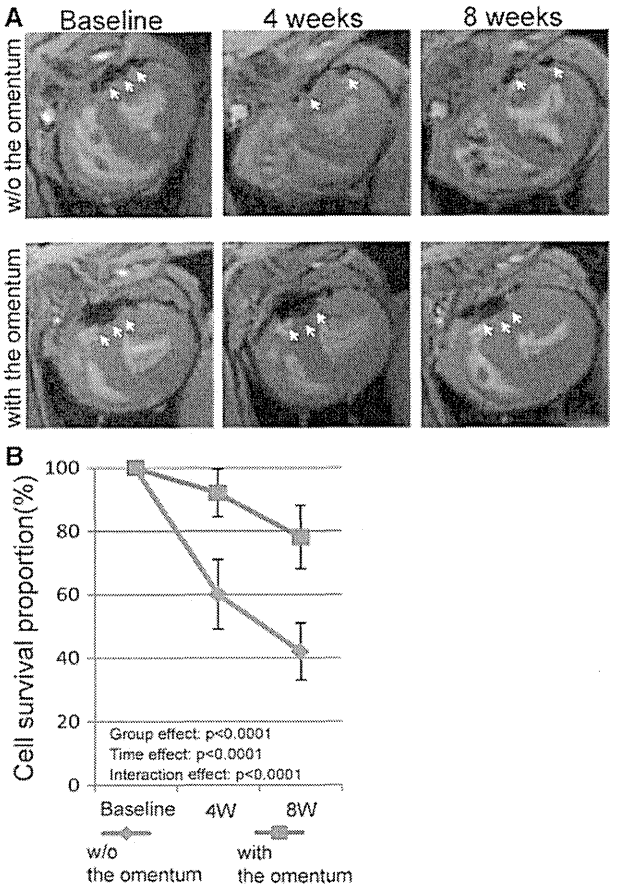

Figure 3. In vivo analysis of the survival of superparamagnetic iron oxide (SPIO)–labeled human induced pluripotent stem cell–derived cardiomyocytes (hiPS-CMs) after transplantation. **A**, Serial cardiac MRIs were examined at 1 week (baseline), 4 weeks, and 8 weeks after SPIO-labeled hiPS-CM cell-sheet transplantation, with or without the omentum. Representative hypointense area of the SPIO-labeled hiPS-CMs is indicated by white arrows. **B**, Cell survival proportion was estimated by the SPIO-labeled area at 4 and 8 weeks, corrected by cell survival at 1 week.

greater in mini-pigs with the omentum (64±21 U/mm^2) than in those without it (9±5 U/mm^2; P<0.0001; Figure 5C).

Upregulation of VEGF, Basic Fibroblast Growth Factor, and SDF-1 Expression in the Transplanted Area

The expression level of cardioprotective and angiogenic factors in the transplanted area at 8 weeks after treatment was quantitatively assessed by real-time polymerase chain reaction for VEGF, basic fibroblast growth factor, and SDF-1. The relative expression of all the factors in the transplanted area was significantly greater in mini-pigs with the omentum than in those without it (VEGF, 1.94±0.38 versus 1.35±0.26; P<0.05; basic fibroblast growth factor, 2.33±0.92 versus 1.21±0.19; P<0.05; SDF-1, 2.05±0.33 versus 1.22±0.21; P<0.01; Figure 6A–6C).

Discussion

It is herein demonstrated that our differentiation protocol yielded hiPS-CMs with >80% purity, and hiPS-CM cell sheets were transplanted over the anterior wall of the ventricle, covered by the pedicle omentum, in a porcine model without procedural failure or procedure-related morbidity/mortality. The number of surviving cTNT-positive hiPS-CMs on the native myocardium was significantly greater in mini-pigs with the omentum than in those without it, although there was a steady decrease in the surviving cell number, regardless of the omentum support, as assessed by SPIO cell labeling with CMR and by immunohistolabeling. The pedicle omentum covering markedly increases the number of vessels and capillaries, associated with the upregulation of VEGF, hepatocyte growth factor, and SDF-1, at the transplanted area compared with the cell-sheet transplantation without the omentum.

In the present study, SPIO-labeled hiPS-CMs were clearly visualized in vivo by CMR, corresponding to the histological findings that confirmed iron contents in the transplanted hiPS-CMs that were positive for cTNT, as reported by previous publications.[22,23] Using this method, the distribution and survival of the transplanted hiPS-CMs were serially evaluated in this study. As a result, it was proved that the unique technique in which transplanted cell sheets were covered by the pedicle omentum elicited a greater survival of the transplanted hiPS-CMs over the ventricular epicardial surface at 4 weeks compared with cell-sheet transplantation without the omentum covering. This suggests that pedicle omentum covering the cell sheets promptly induced angiogenesis to improve the hypoxic environment at the transplanted area, compared with the omentum-free method. In addition, although the size of the graft was decreased in both groups during the 8 weeks, trend in the size reduction was significantly milder in the omentum group than in the omentum-free group. This was consistent to the increased vascular network and upregulated angiogenic factors at the transplanted area in the omentum group at 8 weeks after the cell-sheet transplantation. These findings indicate that covering the cell sheet with the pedicle omentum that carries abundant angiogenic potentials[17–19] enhanced neovascular formation at the transplanted area promptly after transplantation and that vascular-rich structure at the transplanted area persisted long-term. In previous studies, antiapoptotic treatments on the transplanted cells, including upregulation of AKT[24] or overexpression of Bcl-2,[25] have been shown to improve survival after cell transplantation. We achieved to improve cell survival after transplantation by modifying the cell delivery method. The pedicled omental flap is frequently and safely applied for the treatment of mediastinitis after cardiovascular surgery. As cell transplantation is indicated to the patients with severe heart failure, we need to establish a minimally invasive approach to mobilize the omentum. Besides, we expect our unique combination method to be a feasible and safe treatment option in clinical settings. However, in this study, transplanted hiPS-CMs produced by our protocol may be immature, although they were spontaneously contractile. In the specimen 8 weeks after transplantation with the omentum, there were few surviving hiPS-CMs with organized sarcomeres in the cytoplasm, whereas there were many cTNT-positive cells (data not shown). In recent studies, mechanical load of hiPS-CMs in vitro controlled their alignment, proliferation, and hypertrophy,[26] and spontaneous and synchronous beating cardiac cell sheets were created by a bioreactor culture, which expanded and induced cardiac differentiation of hiPS cells.[27] It is necessary to modify